Review

International Journal of Modern Physics B
Vol. 26, No. 18 (2012) 1230010 (57 pages)

DOI: 10.1142/S0217979212300101

World Scientific
www.worldscientific.com

ON ALLOMETRY RELATIONS

DAMIEN WEST* and BRUCE J. WEST†

*Physics Department, Renesselaer Polytechnique Institute, Troy, New York
†Information Sciences Directorate, US Army Research Office,
Research Triangle Park, NC 27709, USA

Received 8 June 2012
Published 6 July 2012

There are a substantial number of empirical relations that began with the identification of a pattern in data; were shown to have a terse power-law description; were interpreted using existing theory; reached the level of "law" and given a name; only to be subsequently fade away when it proved impossible to connect the "law" with a larger body of theory and/or data. Various forms of allometry relations (ARs) have followed this path. The ARs in biology are nearly two hundred years old and those in ecology, geophysics, physiology and other areas of investigation are not that much younger. In general if X is a measure of the size of a complex host network and Y is a property of a complex subnetwork embedded within the host network a theoretical AR exists between the two when $Y = aX^b$. We emphasize that the reductionistic models of AR interpret X and Y as dynamic variables, albeit the ARs themselves are explicitly time independent even though in some cases the parameter values change over time. On the other hand, the phenomenological models of AR are based on the statistical analysis of data and interpret X and Y as averages to yield the empirical AR: $\langle Y\rangle = a\langle X\rangle^b$. Modern explanations of AR begin with the application of fractal geometry and fractal statistics to scaling phenomena. The detailed application of fractal geometry to the explanation of theoretical ARs in living networks is slightly more than a decade old and although well received it has not been universally accepted. An alternate perspective is given by the empirical AR that is derived using linear regression analysis of fluctuating data sets. We emphasize that the theoretical and empirical ARs are not the same and review theories "explaining" AR from both the reductionist and statistical fractal perspectives. The probability calculus is used to systematically incorporate both views into a single modeling strategy. We conclude that the empirical AR is entailed by the scaling behavior of the probability density, which is derived using the probability calculus.

Keywords: Allometry; fractals; physiology; scaling; statistical analysis; ontogenetic growth.

Report Documentation Page

Form Approved
OMB No. 0704-0188

1. REPORT DATE	2. REPORT TYPE	3. DATES COVERED
06 JUL 2012		**00-00-2012 to 00-00-2012**

4. TITLE AND SUBTITLE	5a. CONTRACT NUMBER
On Allometry Relations	5b. GRANT NUMBER
	5c. PROGRAM ELEMENT NUMBER
6. AUTHOR(S)	5d. PROJECT NUMBER
	5e. TASK NUMBER
	5f. WORK UNIT NUMBER
7. PERFORMING ORGANIZATION NAME(S) AND ADDRESS(ES) **Information Sciences Directorate, U. S. Army Research,Office, ,Research Triangle Park,,NC,27709**	8. PERFORMING ORGANIZATION REPORT NUMBER
9. SPONSORING/MONITORING AGENCY NAME(S) AND ADDRESS(ES)	10. SPONSOR/MONITOR'S ACRONYM(S)
	11. SPONSOR/MONITOR'S REPORT NUMBER(S)

12. DISTRIBUTION/AVAILABILITY STATEMENT
Approved for public release; distribution unlimited

13. SUPPLEMENTARY NOTES
See also ADA610492,InternationalJournal of Modern Physics B Vol.26,No.18(2012)1230010(57pages)

14. ABSTRACT

15. SUBJECT TERMS

16. SECURITY CLASSIFICATION OF:			17. LIMITATION OF ABSTRACT	18. NUMBER OF PAGES	19a. NAME OF RESPONSIBLE PERSON
a. REPORT	b. ABSTRACT	c. THIS PAGE			
unclassified	**unclassified**	**unclassified**	**Same as Report (SAR)**	**57**	

1. Introduction

At the turn of the nineteenth century the German polymath Gauss[64] and the American mathematician Adrian[1] introduced into science the law of frequency of errors, the French physicist Laplace[116] proved the central limit theorem and the French zoologist Curvier[34] determined that the brain mass of a mammal increases more slowly than does its total body mass (TBM). Cuvier's observations initiated the field of Allometry that relates the size of an organ to that of the host organism with mass serving as a measure of size. The roads of statistical analysis and observation (experiment) converge in the twenty-first century to explain the origin of allometry relations (ARs).

Allometry, literally meaning by a different measure, has acquired a mathematical description through its relations along with a number of theoretical interpretations to account for its mathematical form. However no one theory has been universally accepted as successfully explaining ARs in their many guises so the corresponding origins remain controversial. Consequently, in reviewing the properties of allometry data along with their various theoretical explanations we herein provide a glimpse as to those origins.

We use the generic term network in our narration in order to slip smoothly from ARs in physical networks with identical particles and van de Waal's forces, to biological networks with structured elements and chemical interactions, to geophysical networks with complex tributaries and branching architectures. This nomenclature also enables us to transition from arcane historical theory to a modern perspectives of complex networks. The mathematics of renormalization group (RG) theory,[103,259] fractional differential equations,[126,144] fractional stochastic differential equations[236] and transitioning from dynamic variables to phase space variables to express the probability calculus in terms of fractional diffusion equations[108,207,236] are herein found to provide insight into different aspects of the origins of ARs.

Allometry has been defined as the study of body size and its consequences[79,176] both within a given organism and between species in a given taxon. Gayon[65] reviewed the history of the concept of allometry, defined as the study of body size and its consequences[79,176] within a given organism and between species in a given taxon, and distinguished between four different forms: (1) ontogenetic allometry, which refers to relative growth in individuals; (2) phylogenetic allometry, which refers to constant differential growth ratios in lineages; (3) intraspecies allometry, which refers to adult individuals within a species; (4) interspecies allometry, which refers to the same kind of phenomenon among related species. The theoretical entailment of static from dynamic allometry models has not been systematically studied, although there has been some recent effort in that direction.[67,243] Herein we review the use of phenomenological dynamic equations from physical biology to relate the dynamic allometry of the first two categories to their static counterparts in the last two.

Galileo[62] recognized that in order for an organism or physical structure to retain a constant function as size increases requires its shape (architecture) and/or the

materials with which it is constructed to change. This simple physical picture has biological and social analogs in which the size of a network has unavoidable consequences.[164,213] We focus on ARs for physiologic phenomena, but we do indicate where insight might also be gained from other disciplines as well.

1.1. *What is the equation?*

Sir Julian Huxley[98]; grandson of the Huxley of Darwin evolution fame, brother of the novelist Aldous (*Brave New World*) and half-brother of the biophysicist Andrew (the Hodgkin–Huxley equations)[209]; proposed that two parts of the same organism have proportional rates of growth. In this way if Y is a living subnetwork observable with growth rate ϑ and X is a measure of the size of a living host network with growth rate γ then the fractional increase in the two is denoted according to Huxley by:

$$dX/\gamma X = dY/\vartheta Y\,. \tag{1}$$

This equation can be directly integrated to obtain:

$$Y = aX^b\,, \tag{2}$$

the time-independent AR where a and b $(= \gamma/\vartheta)$ are empirically determined. The theoretical AR given by Eq. (2) considered by Huxley is the basis of subsequent theoretical discussions in such excellent books as Schmidt–Nielson[195] and Calder.[31]

The intraspecies AR relates a property of an organism within a species to its TBM. The interspecies AR relates a property across species such as the basal metabolic rate (BMR) to TBM.[31,195] These two allometry groups are distinctly different and the models developed to determine the theoretical forms of the allometry coefficient a and exponent b in the two cases are quite varied, as shown subsequently.

Equation (2) looks very much like the scaling relations that have become so popular in the study of complex networks over the last decade.[3,30,153,221,239] Historically the nonlinear nature of Eq. (2) has precluded the direct fitting of the equation to data. A logarithmic transformation is traditionally made and a linear regression to the data on the equation

$$\ln Y = \ln a + b \ln X \tag{3}$$

is used to estimate the parameters a and b. In Sec. 2 we review a myriad of phenomena from a number of disciplines in which ARs have been brought to light. In Sec. 3 we discuss the fitting of ARs to data.

All complex dynamical networks manifest fluctuations, either due to intrinsic nonlinear dynamics producing chaos[124,155] or due to coupling of the network to an infinite dimensional, albeit unknown environment,[118] or both. The modeling strategies adopted to explain ARs have traditionally taken one of two roads: the statistical approach in which residual analysis is used to understand statistical patterns and

to identify the causes of variation in the AR;[31,195] or the reductionist approach to identify mechanisms that explain specific values of the allometry parameters.[10,247] We find that neither approach separately provides a complete explanation of the variety of phenomena described by ARs. The influence of the environment, whether inducing fluctuations in a reductionist model, or producing a systematic change in a statistical model, has been taken into account in multiple studies.[71,73,141] In Sec. 5 we take the road of the probability calculus that systematically incorporates both reductionistic and statistical mechanism into the phenomenological explanation of ARs. This calculus enables modelers to associate characteristics of the measured probability density function (*pdf*) with specific deterministic mechanisms and with structural properties of the coupling between variables and fluctuations.[118,175]

1.2. *Is there universality?*

In physics the notion of universality occurs in the context of critical phenomena, where in the vicinity of a phase transition a network ceases to have a characteristic scale and can be characterized by a set of critical exponents. The principle of universality claims that networks that undergo a phase transition can be grouped into one of a small number of universality classes. Gisiger[68] discusses universality in the context of invariance in biology; specifically addressing the role of $1/f$ noise. In the context of AR universality might imply that the allometry exponent plays the role of a critical exponent. The empirical evidence suggests that this interpretation of the allometry exponent is not appropriate. A somewhat less stringent definition of universality may be defensible; one in which the details of the interactions are washed out but the form of the AR persists with the allometry exponent in a restricted interval.

In biology the ARs associate functional variables with measures of body size, such as the TBM $X = M$ raised to a noninteger power M^b. The average BMR is one such functional variable $Y = B$ that can be expressed in terms of TBM. The most prevalent theories of metabolic allometry argue for either $b = 2/3$, based on body cooling, or $b = 3/4$, based on energy efficiency. Selected data sets have been used by various investigators to support either of these two values. However, there is also strong evidence that there is no universal value of b that is satisfied by all metabolic data. In fact, Bokma[21] presents a large amount of fish data to demonstrate that no single universal value of the allometry exponent b exists. This argument is supported by Glazier[72] who observes that the isometric ($b = 1$) metabolic scaling of pelagic animals is an evolutionarily malleable trait that responds to environmental changes.

On the other hand, West and Brown[252] argue that living networks do have universal scaling laws. Their arguments rest on patterns observed in biological and botanical data and the quantitative theory of the fractal structure, organization and dynamics of the branching networks in living systems. The theory developed by West *et al.*,[247] which we review in Sec. 4, has as one of its tenets the existence of hierarchical fractal-like branching networks for the delivery of nutrients resulting in

$b = 3/4$. They attribute this origin of metabolic AR to evolution's solution to the grand challenge of how highly complex, self-sustaining, reproducing, living networks service enormous numbers of localized microscopic units in an efficient and "democratic" way. Their conclusion, like that of the earlier analysis others,[230,231] was that fractal networks have an evolutionary advantage over those that scale classically,[213] independently of what the networks distribute from macroscopic reservoirs to microscopic sites.

Scaling is a ubiquitous property of large complex networks indicating that the observables simultaneously fluctuate over many time and/or space scales. In the physical sciences such phenomena have historically been categorized as $1/f$ noise[225] or $1/f$ variability.[239] Mandelbrot[131] was probably the first to recognize the wide-ranging significance of this $1/f$ variability with his introduction of fractals into the scientist's lexicon. The existence of ARs has been closely tied to fractal geometry by some investigators[247] and in Sec. 5 we show that the origin of AR may reside in fractal statistics, the scaling of *pdfs*, and not in fractal geometry.

1.3. *Some comments on fractals*

Mandelbrot[131,132] identified ARs masquerading under a variety of empirical "laws" and argued that they were a consequence of complex phenomena not having characteristic scales. Subsequent interpretations of ARs often involve fractals and so we recall some fundamental properties of fractals that are subsequently useful. To begin let us give a qualitative definition of a fractal:[133] "A fractal is a shape made of parts similar to the whole in some way."

The fractal concept arises in three distinct, but related guises; geometry, statistics and dynamics. Geometric fractals deal with the self-similarity of complex geometric forms. A fractal object examined with ever increasing magnification reveals ever greater levels of detail; detail that is self-similar in character. The basic mathematical properties of geometric fractals and their myriad of applications can be found in a number of excellent books[17,55,57,131,133,143,238] and is not repeated here. We merely record and interpret those properties that may be needed for the analyses of ARs. The number of self-similar objects N required to cover an object of dimension D is given by $N = r^{-D}$, where r is the size of the "ruler". In this way the fractal dimension of the object being covered can be mathematically defined as:

$$D = -\ln N / \ln r \tag{4}$$

in the limit of vanishing r. As the ruler size goes to zero the number of rulers necessary to cover the object diverges to infinity in such a way that D remains finite for self-similar objects and this dimension is not necessarily integer valued.

An observable $Z(t)$ is scaling if for a positive constant c it satisfies the homogeneity relation

$$Z(ct) = c^H Z(t)\,. \tag{5}$$

Modifying the units of the independent variable therefore only changes the overall observable by a multiplicative factor; this is self-affinity. Barenblatt[13] remarked that such scaling laws are not merely special cases of more general relations; they never appear by accident and they always reveal self-similarity. Note that scaling alone is not sufficient to prove that a function is fractal, but if a function is fractal it does scale.

In the sequel we relax the distinction between self-affine and self-similar, since self-similarity has been extended to encompass both meanings in the physics literature. Meakin[143] asserts that in homogeneous scaling relations it is the coefficient that embodies the "real physics" behind power-law relations. He further observed that the allometry exponents are universal in many homogeneous scaling phenomena and the allometry coefficients provide the only means to control physical properties and behavior.

Scale invariance or scaling requires that a function $\Phi(X_1, \ldots, X_N)$ be such that scaling each of the N variables by an appropriate choice of exponents $(\alpha_1, \ldots, \alpha_N)$ always recovers the same function $\Phi(X_1, \ldots, X_N)$ up to an overall constant:

$$\Phi(X_1, \ldots, X_N) = \gamma^{\beta} \Phi(\gamma^{\alpha_1} X_1, \ldots, \gamma^{\alpha_N} X_N)\,. \tag{6}$$

We observe that Eq. (2) is possibly the simplest of such scaling relations between two variables such that they satisfy the RG relation

$$X(\gamma Y) = \gamma^{b} X(Y)\,.$$

The lowest-order solution to this equation is, of course, given by Eq. (2) and we provide the general solution subsequently. Changes in the host network X (size) control (regulate) changes in the subnetwork Y (property) in living networks and in some physical networks through the homogeneous scaling relation.

Inhomogeneity in space and intermittency in time are the hallmarks of fractal statistics and it is the statistical rather than the geometrical sameness that is evident at increasing levels of magnification. In geometrical fractals the observable scales from one level to the next. In statistical fractals where the phase space variables (z, t) replaces the dynamic variable $Z(t)$ it is the *pdf* $P(z, t)$ that satisfies a scaling relation:

$$P(\alpha z, \beta t) = \beta^{-\mu} P(z, t)\,; \quad \mu = \ln \alpha / \ln \beta\,, \tag{7}$$

where $\mu = 2H$ and the homogeneity relation is interpreted in the sense of the *pdf* in Eq. (7). Time series with such statistical properties are found in multiple disciplines including finance,[134] economics,[135] neuroscience,[4,226] geophysics,[215] physiology[240] and general complex networks.[244] A complete discussion of statisical data with such scaling behavior is given by Beran[20] in terms of the long-term memory captured by the scaling exponent. One example of a scaling *pdf* is given by:

$$P(z, t) = \frac{1}{t^{\mu}} F_z \left(\frac{z}{t^{\mu}} \right) \tag{8}$$

and in a standard diffusion process $Z(t)$ is the displacement of the diffusing particle from its initial position at time t, $\mu = 1/2$ and the functional form of $F_z(\cdot)$ is a Gauss distribution. However, for general complex phenomena there is a broad class of distributions for which the functional form of $F_z(\cdot)$ is not Gaussian and the scaling index $\mu \neq 1/2$, see Sec. 5 for additional discussion.

Dynamic fractals do not directly enter our discussion of ARs. However for completeness we mention that in a dynamic fractal the geometry of the manifold on which the dynamics of a network unfolds is fractal, so that the associated chaotic time series is also fractal.[155]

2. Empirical Allometry

In this section we review areas of investigation where size has been observed to control the properties of a phenomenon. In so doing we catalog a number of phenomenological relations that are not often discussed from the same perspective. There is a nontrivial number of empirical relations that began as the identification of a pattern in data; were shown to have a terse power-law description; were interpreted using existing theory; reached the level of "law" and given a name, not always after the discoverer; only to subsequently fade away when it proved impossible to connect the "law" with a larger body of theory and/or data. An example drawn from the *Notebooks* of Leonardo da Vinci[177] relates the diameter of a parent limb d_0 to two daughter limbs d_1 and d_2 :

$$d_0^\alpha = d_1^\alpha + d_2^\alpha \,. \tag{9}$$

The da Vinci scaling relation supplies the phenomenological mechanism necessary for AR to emerge in a number of disciplines, as we subsequently discuss.

Nearly five hundred years after de Vinci recorded his observations Murray[150] used energy minimization to derive the same equation with the theoretical value $\alpha = 3$, which is known in the literature as Murray's Law or the Murray–Hess Law. In the simplest case $d_1 = d_2$ the da Vinci scaling relation reduces to scaling between sequential generations of a bifurcating branching network having daughter branches of equal radii:

$$d_{k+1} = 2^{-1/\alpha} d_k \tag{10}$$

resulting in an exponential reduction in branch diameter from generation to generation.

2.1. *Living networks*

Living networks have static intraspecies ARs that link two distinct but interacting parts of the same organism in terms of mass, with mass serving as a measure of size. Smith[202] maintained that concentrating on a power function as the method for evaluating the biological consequences of size has masked the complexity ofthe

allometry problem. We agree with this observation, but perhaps in ways that Smith would not have anticipated, as will become evident.

2.1.1. *Biology*

Cuvier[34] was the first to recognize that brain mass increases more slowly than TBM as we proceed from small to large species within a taxon. This empirical observation was subsequently made between many other biological observables and was first expressed mathematically as an allometric relation by Snell[204]:

$$\text{brainweight} = a(\text{bodyweight})^b\,, \tag{11}$$

where on log–log graph paper a is the intercept with the vertical axis and b is the slope of the line segment. Mammalian neocortical quantities Y have subsequently been empirically determined to change as a function of neocortical grey matter volume X as an AR. The neocortical allometry exponent was first measured by Tower[214] for neuron density to be approximately $-1/3$. The total surface area of the mammalian brain was found to have an allometry exponent of approximately $8/9$.[94,100,167] Changizi[33] points out that the neocortex undergoes a complex transformation covering the five orders of magnitude from mouse to whale depicted in Fig. 1 but the ARs persist; those mentioned here along with many others.

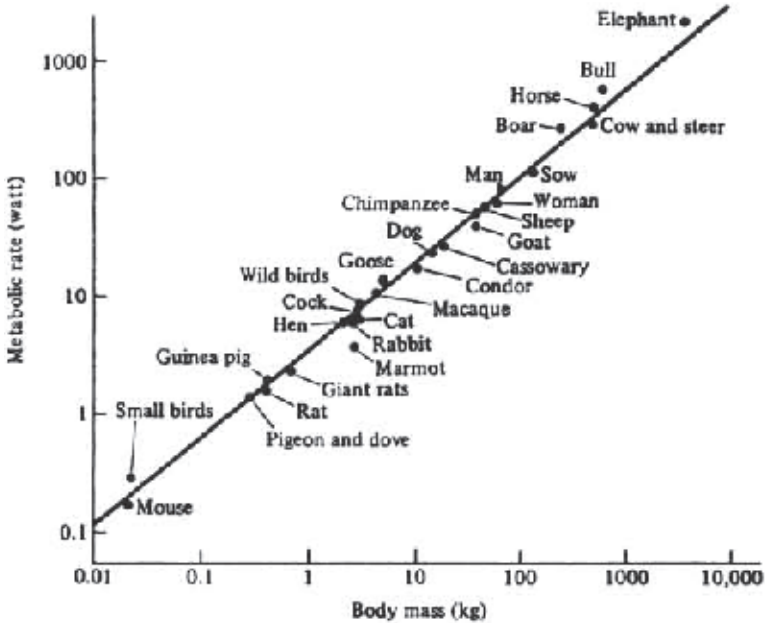

Fig. 1. Mouse to elephant curve. BMR of mammals and birds are plotted versus TBM on log–log graph paper. The solid line sement is the best linear regression of Eq. (2) to the data with a slope very close to 3/4. [reproduced from Schmidt–Nielsen[195] with permission].

Another quantity of interest is the time; not the chronological time measured by a clock but the intrinsic time of a biological process first called biological time by Hill.[93] Hill reasoned that since so many properties of an organism change with size that time itself may scale with TBM. Lindstedt and Calder[119] develop this concept further and determine experimentally that biological time, such as species longevity, satisfies an AR with Y being the biological time. Lindstedt *et al.*[121] clarify that biological time τ is an internal mass-dependent time scale

$$\tau = aM^b \tag{12}$$

to which the duration of biological events are entrained. They present a partial list of such events that includes breath time, time between heart beats, blood circulation time and time to reach sexual maturity. In all these examples and many others the allometry exponent clusters around the theoretical value $b = 1/4$. Note that the total energy of an organism seen as a bioreactor is proportional to volume (M) and the biological time is proportional to $M^{1/4}$, so the metabolic rate (energy/time) would scale as $M^{3/4}$.

2.1.2. *Botany*

Niklas[154] shows in Fig. 2 an impressive statistical trend spanning twenty orders of magnitude in the mass of aquatic and terrestrial nonvascular and vascular plant species. The annual growth in plant body biomass G_T (net annual gain in dry mass per individual) and M_T (total dry mass per individual) are related by the

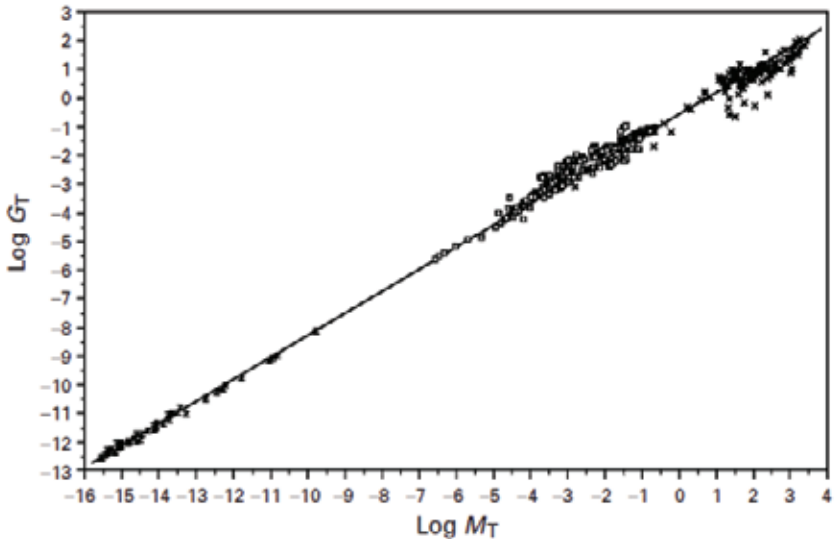

Fig. 2. Log–log bivariate plot of total annual growth rate in dry body mass per individual G_T versus TBM. Line segment denotes reduced major axis regression curves for the entire data set. [adapted from Niklas[154] with permission].

empirical AR:

$$G_T \propto M_T^{3/4} . \tag{13}$$

Figure 2 shows linear regression on logarithmically transformed data

$$\log G_T = \log a + 0.75 \log M_T \tag{14}$$

and the parameter a is the intercept with the vertical axis. In the data analyses recorded herein the terms weight, mass and volume are used almost interchangeably as measures of size. The allometry exponent is 3/4 for the data in Fig. 2 but empirically differs from this value when the data sets are graphed individually. The allometry coefficients of the separate data sets may vary as a function of habitat as well. The agreement between the biomass data and the AR with exponent 3/4 is very suggestive but it must be viewed critically because of methodological limitations.

Reich *et al.*[174] analyzed data for approximately 500 observations of 43 perennial plant species of coupled measurements of whole-plant dry mass and G_T from four separate studies. Collectively, the observations span five of the approximately 12 orders of magnitude of size in vascular plants.[53] The result of each experiment yielded an isometric scaling of $b \approx 1$ and not $b = 3/4$ as did the scaling of G_T to TBM for whole plants. Consequently, even when data look as appealing as they do in Fig. 2 things are not always what they seem.

2.1.3. *Clearance curves*

Another allometry phenomenon is the dependence of drug-dosing range on TBM and is referred to as clearance.[97] Zenobiotic clearance is the rate at which any foreign compound not produced by an organism's metabolism is passed from the organism. The application of allometry ideas to pharmacokinetics and to determining human parameters from those in animals is fairly recent.[22,127,191] The early studies did not address questions of variability in the allometry parameters and were primarily concerned with whether the allometry exponent more closely tracked the value 2/3 or 3/4 by doing linear regression on log-transformed data.[122]

Hu and Hayton[97] addressed the possible impact of statistical variability in the AR parameters on the predicted pharmacokinetic parameter values. They found considerable uncertainty in the value of the allometry exponent, which they fit to a Gaussian distribution with mean value 0.74. Even though they could not determine whether the variability in the allometry exponent was due to experimental error or to biological mechanisms they did find that there was no systematic deviation from the AR. However it appears that whether $b = 3/4$ or 2/3 depends on which of the major elimination pathways is used, metabolism for the 3/4 value and renal excretion for the 2/3 value.

2.1.4. *Physiology*

The most studied of the interspecific ARs does not concern relative growth but is that associating the average BMR measured in watts to average TBM measured in kilograms of multiple species such that:

$$B = aM^b\,. \tag{15}$$

The metabolic rate refers to the total utilization of chemical energy for the generation of heat by the body of an animal and is often measured by the oxygen intake during respiration.

The earliest physiologic model for the value of the allometry exponent in the intraspecies AR was given by Sarrus and Rameaux.[188] Schmidt–Nielsen[195] records that this team of a mathematician and a physician reasoned that the heat generated by a warm blooded animal is proportional to the volume and the heat loss is proportional to the animal's free surface. Experiments on dogs by Rubner[183] supported their argument and lead to the wide acceptance of the "surface law" in which $b = 2/3$. In Fig. 1 the "mouse-to-elephant" curve depicts the BMR for mammals and birds plotted versus TBM on log–log graph paper spanning six orders of magnitude. The solid line segment is the fit of the AR to the data and yields the empirical value $b \approx 3/4$.

As Niklas[154] noted the expectation was that the metabolic rate would be proportional to the 2/3 power of the TBM as prescribed by the surface law. Surprisingly, this turned out not to be the case. The research of Kleiber[109] and Brody[24] revealed that the slope was closer to 3/4 than to 2/3. Subsequent observational studies have reinforced the allometric pattern observed in the data predicted by Eq. (15) including some relating the 3/4-rule to plants, see, for example, Hemmingsen.[86] Consequently the phenomenological value of the allometry exponent b remains controversial.[47,71,91]

Controversy also persists regarding the theoretical explanation as to why the allometry exponent b should have a specific value. The simple geometrical argument of Sarrus and Rameaux suggests $b = 2/3$ as reviewed in a number of excellent sources.[31,47,91] On the other hand, the quarter-power AR is explained by West, Brown and Enquist (WBE) using geometric scaling arguments from fractal physics to establish the value $b = 3/4$ and other quarter-power scaling laws in physiology, see Sec. 4.

Heusner[91] adopted geometric scaling arguments to obtain $b = 2/3$ in the AR between BMR and TBM. He argued that the various other values experimentally observed for the power-law index by investigators are a consequence of differing values of the allometric coefficient a. He reasoned that two or more data sets with $b = 2/3$ but with different values of a graph as parallel line segments on log–log graph paper, but when the two or more data sets are grouped together and analyzed as a single data set the aggregate is fit by a single line segment with net slope $b > 2/3$. The same argument can be found in a number of other references.[176,195] But unlike those earlier references Heusner[91] concluded that it is the allometry

coefficient that remains the central mystery of allometry and not the allometry exponent. We investigate the implications of Heusner's conjecture in Sec. 3 where we numerically explore the implications of treating the allometry coefficient as a random variable.

It is useful to list the various forms of physiological allometry given by Lindstedt and Schaeffer[122]: pulmonary and cardiac allometry with $b = -1/4$; renal allometry with $b = -0.85$; liver allometry with $b = -0.85$; pulmonary blood volume with $b = 1.0$; cardiac output with $b = 3/4$ and pulmonary transit times with $b = 1/4$.

2.1.5. *Information transfer*

There are literally dozens of physiologic ARs for physiologic time τ, relative to clock time t, that increases with increasing body size $\tau = aM^{b}$[120] and describes chemical processes such as the turnover time for glucose with $b = 1/4$[9] to the life span of various animals in captivity with $b = 0.20$.[185] Schmidt–Nielsen[195] explains how a variety of physiologic time scales such as the length of a heart beat and respiration all scale with body size and from that deduce a number of interesting relations. It is only recently however that Hempleman *et al.*[88] hypothesized a mechanism to explain how information about the size of an organism is communicated to the organs within the organism. Their hypothesis involved matching the neural spike code to body size to convey this information.

Hempleman *et al.*[88] suggest that mass-dependent scaling of neural coding may be necessary for preserving information transmission with decreasing body size. They point out that action potential spike trains are the mechanisms for long distance information transmission in the nervous system. They go on to say that neural information may be "rate coded" with average spike rate over a time period encoding stimulus intensity or "time coded" with the occurrence of a single spike encoding the occurrence of a rapid stimulus transition. The hypothesis is that some phasic physiological traits are sufficiently slow in large animals to be neural rate coded, but are rapid enough in small animals to require neural time coding. These trait include such activities as breathing rates that scale with $b = -1/4$.

They tested for this allometry scaling of neural coding by measuring action potential spike trains from sensory neurons that detect lung CO_2 oscillations linked to breathing rate in birds ranging in body mass from 0.045 to 5.23 kg. While it is well known that spike rate codes occur in the sensing of low frequency signals and spike timing codes occur in the sensing of high frequency signals, their experiment was the first designed to test the transition between these two coding schemes in a single sensory network due to variation in body mass. The results of their experiments on breathing rate was an allometry exponent in the interval $-0.26 \leq b \leq -0.23$ and although taken on a small number of birds their results do suggest a preservation of information transmission rates for high frequency signals in intrapulmonary chemoreceptors and perhaps other sensory neurons as well. The implications of these experiments strongly suggest the need to continue such investigations.

On the more theoretical side Moses *et al.*[149] apply the scaling ideas of metabolic allometry developed by West *et al.*[247] to information networks consisting of microprocessors to form a network. Moses *et al.*[149] use a fractal argument to construct a two-dimensional hierarchal self-similar branching network, an H-tree that Mandelbrot[131] originally used in his discussion of the space filling behavior of the human lung. They show that this branching network of microprocessors have a striking similarity to such networks in organisms even though the latter has evolved by natural selection and the former are designed by engineers.

Along this same line E. F. Rent, while an IBM employee in the 1960s, wrote a number of internal memos (unpublished) relating the number of pins at the boundaries of an integrated circuit (X) to the number of internal components (Y), such as logic gates, to obtain an AR with $b < 1.0$. This rule has historically been used by engineers to estimate power dissipation in interconnections and for the placement of components in very large scale integrated (VLSI) circuit design. More recently Rent's Rule has been used to model information processing networks in the human brain[16] where the mass of grey and white matter are shown to satisfy an AR as first noted by Schlenska.[194] Beiu and Ibrahim[18] suggested that the allometry exponent for grey and white matter between species is identical to the Rent exponent within a species and this was supported using MRI data by Bassett *et al.*[16]

2.2. *Physical networks*

Some of the oldest ARs involve physical networks, or more specifically geophysical networks. The skeptic need only return to da Vinci's scaling relation. In his notebooks da Vinci explains the meaning of this equation not only in the context of relating tree trunks to subsequent branches, but to the branchings of rivers as well. Long before the conservation of energy and the continuity of fluid flow were known to scientists, the enigmatic Italian painter, sculptor, military engineer and anatomist understood the basics of hydrologic networks.

2.2.1. *Geology and geomorphology*

Horton's law of river numbers is another empirical regularity observed in the topology of river networks.[95] As observed by Scheidegger[192] the number of river segments in successive order form a geometrical sequence such that, the

$$\text{number of rivers with } k \text{ tributaries } \propto R_b^{1-k}. \tag{16}$$

The bifurcation parameter R_b is the constant ratio between successive numbers of river networks, known as Horton's law of stream numbers $n_k/n_{k+1} = R_b$ and has the empirical value between 4.1 and 4.7 in natural river networks,[159,160] in contrast to the random model that predicts a value of four. Note that the system of counting begins at the smallest tributary that are the most numerous $R_b > 1$ and these feed into larger tributaries that are fewer in number.

Dodds and Rothman[46] point out that universality arises when the qualitative character of a network is sufficient to quantify its essential features, such as the exponents that characterize scaling laws. They go on to say that scaling and universality have found application in the geometry of river networks and the statistical structure of topography within geomorphology. They maintain that the source of scaling in river networks and whether or not such scaling belongs to a single universality class is not yet known. They do provide a critical analysis of Hack's law, see also, Rodriguez–Iturbe and Rinaldo.[182]

2.2.2. *Hydrology*

Hack's law is a hydrologic AR having to do with the drainage basins of rivers. Hack[83] developed an empirical relation between mainstream length of a river network and the drainage basin area at the closure of the river. Hack's law is given by,

$$\text{mainstreamlength} \ \propto (\text{area})^h \,, \tag{17}$$

where h is the Hack exponent with the typical empirical value $h \approx 0.57$. Hack asserted that river networks are not self-similar.

Mandelbrot[131] relates Hack's exponent to the fractal dimension of the river network and debates the interpretation of the equation. Feder[57] observed that defining a fractal dimension for river networks was obscure and required further study. A modern version of this discussion in terms of hydrologic allometry is given by Rinaldo *et al.*[181] who point out that optimal channel networks yield $h = 0.57 \pm 0.02$ suggesting that *feasible optimality*[178] implies Hack's law. Another viable model is given by Sagar and Tein[186] that is geomorphology realistic giving rise to general ARs in terms of river basin areas, as well as parallel and perpendicular channel lengths.

Maritan *et al.*[136] consider an analogy with the metabolic AR using $M \propto B^\alpha$, that is, $\alpha = 1/b$ so that $\alpha = 1 + h$ with the limiting values $\alpha = 3/2$ and $h = 1/2$ in the case of geometric self-similarity. Geometric self-similarity is the preservation of the river's shape as the basin increases in area. The observed values lie in the range $1.5 \leq \alpha \leq 1.6$ and the scatter of individual curves (analog of intraspecies data) is remarkably small. These values suggest that the branching nature of rivers is fractal, that is, $\alpha > 3/2$ in most cases. The ensemble average of Hack's exponents from different basins extend over 11 orders of magnitude and is indistinguishable from $h = 1/2$.[146] Maritan *et al.*[136] conclude that like the interspecies metabolic rate, the slope of the intraspecies h's are washed out in the ensemble average, resulting in the value $h = 1/2$.

2.3. *Natural History*

Natural History embraces the study, description and classification of the growth and development of natural phenomena. The focus of investigation includes such

important contemporary areas as ecology and paleontology, parts of which rely heavily on AR and scaling.

2.3.1. *Ecology*

Ecology is the scientific study of the distribution, abundance and relations of organisms and their interactions with the environment. Such living networks include both plant and animal populations and communities along with the network of relations among organisms of different scales of organization. Of concern to us here are the species traits determined by body size and how these in turn affect food web stability. Woodward *et al.*[261] along with many others point out that the largest metazoans, for example, whales (10^8 grams) and giant sequoias, weigh over 21 orders of magnitude more than the smallest microbes (10^{-13} grams).[102,234] They go on to stress the considerable variation in body mass among members of the same food web.

We do not address the traditional linking of species through such mechanisms as the prey–predator relation within food webs[76] but instead we focus on body size. The significance of body size has been systematically studied in ecology.[27,35,102] Indentifying X with species abundance and Y with TBM in Eq. (2) there is, in fact, an AR between the species at the base of a food web and the largest predator at the top.[35] We note that species-area power functions have a vital history in ecology[166,258] even though the domain of sizes over which the power law appears valid is controversial.[25,256]

Woodward *et al.*[261] emphasize that AR has been used to explain the observed relations between body size and each of: home range size, nutrient cycling rates, numerical abundance and biomass production. They speculate that body size may capture a suite of covarying species traits into a single dimension, without the necessity of having to observe the traits directly.

Brown *et al.*[26] discuss the universality of the documented ARs in plants, animals and microbes; to terrestrial, marine and freshwater habitats; and to human-dominated as well as "natural" ecosystems. They emphasize that the observed self-similarity is a consequence of a few basic physical, biological and mathematical principles; one of the most fundamental being the extreme variability of the data. The variety of distributions of allometry coefficients and exponents are discussed both phenomenologically and theoretically in subsequent sections.

Farr's law[29] is an example of the change in ARs in the transition from organismic to environmental allometry. Farr collected data on the number of patients committed because of their mental condition and their mortality from a variety of asylums in 1830s England.[56] From these humble beginnings he was able to summarize the "evil effect of crowding" into a relation between mortality rate R and population density ρ[96]:

$$R = a\rho^b \,. \tag{18}$$

Here we see that the size measure used in the metabolic AR, the mass, is replaced with a measure of community structure, the population density. The ARs that capture life histories in ecology and sociology are often expressed in terms of numbers of animals and areas in addition to body mass. Calder[31] points out that size and time seem to be the principle characteristics of life history and ecology.

The factors necessary for the formation of social groups with a restricted geographic area are not understood, but certain ARs help clarify them. The population density ρ of herbivorous mammals has been determined to be related to their mass M by[39] $\rho^{-1} = cM^{0.75}$ where the animals freely roam on a "home range" of given area: $A_{\rm hr} = c'M^{1.02}$. A similar relation exists for carnivores.[145] Consequently, as explained by Calder,[31] herbivorous mammals above a certain size range over an area greater than their per capita share of the local habitat. The degree of overlap was empirically determined to be[40] $A_{\rm hr}\rho = c''M^{0.34}$, where the empirical exponent 0.34 ± 0.11 is statistically indistinguishable from that obtained by combining the separate exponents for the population density and area, that being, $1.02-0.75 = 0.27$. Calder conjectures that the greater the product $A_{\rm hr}\rho$ the greater the intensity of competition and the greater the desirability of social networks that contribute to mutual tolerance within these groups. Makarieva *et al.*[129] argue that animal home range represents a biological footprint of the undisturbed state of an econetwork, however the population density adapts to disturbances in the econetwork. Consequently, the deviation of the home range-population product from isometry reflects the degree of econetwork disturbance.

The AR between maximum abundance and body size for terrestrial plants $N \propto M^{-b}$ was extended by Belgrano *et al.*[19] to the maximum population densities of marine phytoplankton with $b = 3/4$. They draw the implication that maximum plant abundance is constrained by rates of energy supply in both terrestrial and marine networks as dictated by a common AR. Earlier investigators found $b > 3/4$.[37,49]

2.3.2. *Zoology and acoustics*

Mice squeak, birds chirp and elephants trumpet due to scaling. Fitch[59] discusses the relationship between an organism's body size and acoustic characterization of its vocalization under the rubric of acoustic allometry. Data indicate an AR between palate length (the skeletal proxy for vocal tract length) and body mass for a variety of mammalian species. He shows that the interspecies allometry exponent attains the geometric value of three in the regression of skull length and body mass, whereas the intraspecies allometry exponent varies a great deal. The significant variability in the intraspecies allometry exponent suggest taxon-specific factors influencing the AR.[137,199]

Fitch[59] gives the parsimonious interpretation that the variability in the intraspecies allometry exponent could be the result of each species adopting allometric scaling during growth as postulated by Huxley, with a different proportionality

factor for each species. On the other hand, the interspecies allometry exponent could result from the common geometric constraints across species due to the wide range of body sizes. He concludes that the AR between vocal tract dimensions and body size could provide accurate information about a vocalizer's size in many mammals.

2.3.3. *Paleontology*

Pilbeam and Gould[164] provide reasons as to why body size has played such a significant role in biological macroevolution. The first is the statistical generalization known as Cope's Law or Rule, which states that population lineages increase in body size over evolutionary time scales,[36] that is, the body size of a species is an indication of how long it has survived on geological time scales. A second reason is the one mentioned earlier, Galileo's observation that large organisms must change shape in order to function in the same way as do their smaller prototypes.

One quantitative measure of evolution is the development of the brain in mammals at various stages of evolution. Jerison[99] showed that the brain-body relation given by Eq. (2) is satisfied by mammals with an exponent that is statistically indistinguishable from 2/3. He suggested that a may be an appropriate measure of brain evolution in mammals as a class, following the proposal of Dubois[48] that a quantitative measure of cephalization in contemporary mammals be based on the ratio; $a = \text{brain weight}/(\text{body weight})^b$. These hypotheses were directly tested by Jerison[99] using endocranial volumes and body volumes for fossil mammals at early and intermediate evolutionary stages. The data did in fact support the hypothesis.

White and Gould[253] emphasize in their review of the meaning of the allometry coefficient a that it had generated a large and inconclusive literature. Reiss[176] notes that if brain mass is regressed on TBM across individuals in a species the slopes are shallower than of regressions calculated across mean values for different species within a single family (genus). This argument had also been presented by Gould[80] who emphasized the importance of the allometry coefficient in the geometric similarity of allometric growth. This interpretation of the allometry coefficient was at odds with the belief of the majority of the scientific community at the time that the allometry coefficient was independent of body size. This latter view is also contradicted by the data analysis in Sec. 3.

Allometry has been used by Alberch *et al.*[2] as the first step in creating a unifying theory in developmental biology and evolutionary ecology in their study of morphological evolution. They demonstrate how their proposed formalism relate changes in size and shape during ontogeny and phylogeny.

3. Data Statistics

In this section the phenomenology of analyzing AR measurement using statistics is discussed; collecting data, identifying patterns (laws) in the data and developing

methods of statistical analysis. Warton *et al.*[220] point out that fitting a line to a bivariate data set is not a simple task and the AR literature is filled with debate over the proper methodology. Sir Julian readily adopted the statistical approach of linear regression to Eq. (3) on multiple data sets to determine the allometry coefficient a and exponent b. The sophisticated statistical techniques such as principle component analysis were not available to Sir Julian and although they can be found in the modern AR literature least-square regression still appears to be the method of choice.[73,189]

Measures of complex phenomena always contain uncertainty and the data sets invariably fluctuate from measurement to measurement. Thus, $X(t)$ and $Y(t)$ are stochastic variables, and by implication $X(Y)$ is a random function of its argument as well. Consequently the deterministic algebraic equations relating network size and network function never unambiguously represent what is actually being measured. Subsequently, we examine the corresponding mathematical modeling, shifting the focus from the dynamic stochastic variable to the associated dynamic *pdf*.

We examine the phenomenology of the random data from measurements of various properties of allometry networks that determine empirical ARs. In particular we focus on how allometry coefficients and exponents are interpreted given that the data on which they are based fluctuate to such a large extent. Part of the reason for taking this approach is that a significant number of scientists adopt the viewpoint that fluctuations reflect lack of control and/or ignorance about what is being measured. Here we adopt the more sympathetic view that networks are generically random because they are dynamic and complex in which case statistics provide information about the fundamental nature of that complexity.

3.1. *Fluctuations*

All complex dynamic networks are stochastic, either due to intrinsic nonlinear dynamics producing chaos,[123,124,155] or due to coupling of the network to an infinite dimensional albeit unknown environment,[118] or both; completely aside from measurement errors. Consequently, it is necessary to understand how statistical uncertainty may be included in modeling allometry data. Kaitaniemi[104] pointed out that the potential information content of the allometry coefficient has been largely neglected, an observation also made by Glazier[73] among others. Kaitaniemi examined the different ways this parameter may vary for different sources of random fluctuations. Here we follow a similar strategy, but we use actual data rather than computer generated random fluctuations.

The normal or Gauss *pdf* suggests that the statistical variations between the variables in the AR Eq. (2) may be additive leading some scientists[70,130,203] to propose the form:

$$Y = \bar{a}X^{\bar{b}} + \eta\,, \tag{19}$$

where η depicts the random fluctuations and the overbars denote the fitted values of the parameters. Packard and Boardman[157] also investigate the regression of data to a three-parameter power law that does not pass through the origin

$$Y = Y_0 + \bar{a}X^{\bar{b}} + \eta\,. \tag{20}$$

In the near isometry case where $\bar{b} \approx 1$ linear regression analysis is appropriate and additive fluctuations provide a satisfactory representation of the statistical variability. On the other hand when the allometry exponent is substantially different from unity the determination of the nature of the fluctuations requires preliminary statistical analysis, see, for example, Packard.[156]

Packard and Boardman[157] emphasize that the additive form of fluctuations in ARs is quite different from the situation involving the logarithmically transformed data. For the transformed data introducing additive random fluctuations yields:

$$\log Y = \log \bar{a} + \bar{b} \log X + \eta\,, \tag{21}$$

and the empirical constants $\bar{a}$ and $\bar{b}$ are fit to the transformed data. In terms of the original AR we obtain:

$$Y = \bar{a}e^{\eta}X^{\bar{b}} \tag{22}$$

with the fluctuations being exponentially amplified through e^{η}. It is evident that when the fluctuations are considered to be focused in the allometry coefficient, as they are here, they are multiplicative. The multiplicative character of the fluctuations implies that the influence of the random variations is amplified far beyond their additive cousins.

They emphasize that the focus of the research on log-transformed data is to characterize patterns of variation in morphology, physiology and ecology in organisms spanning a broad range in body size in an attempt to identify underlying principles in the design of biological networks, see, for example, Brown *et al.*[27] and references therein. They go on to assert that many of the patterns identified by this research are inaccurate and misleading and these mischaracterizations likely contribute to the ongoing debate about ways in which animals are constructed.

We saw that fluctuations in the log-transformed data may be equivalent to multiplicative fluctuations in the original data. So the important question is whether it is necessary to perform the logarithmic transformation at all. Packard and Boardman[157] point out that the original motivation for the log-transform was to linearize the equations thought to represent the data and therefore facilitate the implementation of graphical and statistical analysis.[162,203] However, they go on to show the biasing problems associated with log-transforms using computer generated data sets and caution that with the present day computer software for fitting nonlinear equations linearization is no longer a sufficient rationale for log-transforms. So are there other reasons to transform the data?

Kerkhoff and Enquist[106] strongly disagree with the conclusions of Packard (2008) that standard methods for fitting allometry models produce "biased and

misleading" results. They point out that most biological phenomena are inherently multiplicative[63,66] and it is the proportional rather than absolute variation that matters. The multiplicative influence of noise seen in the log-transformed data is often misinterpreted as bias.[203,263] Kerkhoff and Enquist[106] maintain that the multiplicative error model is an appropriate feature, rather than a defect, of standard allometry analysis. Recent research suggests that geometric error resulting from multiplicative fluctuations should be the default standard for parameter estimation in biology[66,81] and not additive error.

3.2. *Phenomenological distributions*

We now consider the statistics of the fluctuations in the AR using data from the literature. The data relating the average energy expended by a given species in watts to the average TBM of that species in kilograms for 391 species of mammal is plotted in Fig. 3 and also in Heusner[91] as well as in Dodds *et al.*[47] A fit of Eq. (3) to these data that minimizes the mean-square error is a straight line on double logarithmic graph paper and was found to have slope $\bar{b} = 0.71 \pm 0.008$ so that empirically $2/3 < \bar{b} < 3/4$ and the allometry coefficient $\bar{a} = 0.02$. As West and West[245] reviewed Heusner[90] had somewhat earlier questioned Kleiber's value of 3/4 and concluded from data analysis that this value of 3/4 was a statistical artifact. Feldman and McMahon[58] agreed with Heusner's conclusions, but suggested that there was no compelling reason for the intraspecies and interspecies allometric exponents to be the same, with the intraspecies exponent being 2/3 based on geometric similarity and the interspecies exponent being 3/4 based on McMahon's elastic similarity.

There is a great deal of variability around the line segment that gives the AR model in Fig. 3. West and West[245] interpret these fluctuations as random variations

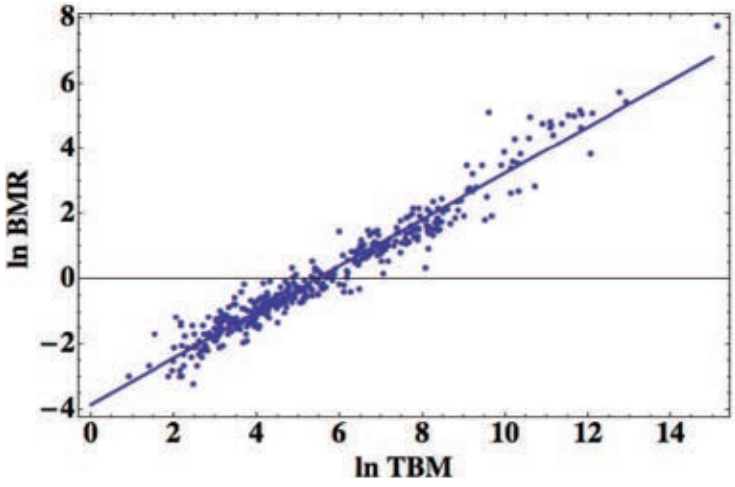

Fig. 3. The linear regression to Eq. (3) for Heusner's data[91] is indicated by the line segment. The slope of the dashed line segment is 0.71 ± 0.008.

in either the allometry coefficient or the allometry exponent. If the fluctuations are assumed to be contained in the allometry coefficient we can define

$$\frac{a}{\bar{a}} = e^{\eta} = \frac{B}{\bar{a}M^{\bar{b}}} \tag{23}$$

so that each data point in the (X, Y)-plane yields a single value of the allometry coefficient. In a complex network a linear response such as suggested by Fig. 3 does not necessarily occur since there can be independent fluctuations in both X and Y resulting in what Warton *et al.*[220] call equation error; also known as natural variability, natural variation and intrinsic scatter. In the present case the AR is not predictive, but instead summaries vast amounts of data.[255] This natural variability is manifest in fluctuations in the allometry parameters (a, b).

West and West[242] calculate the statistical distribution for the random allometry coefficient determined from Eq. (23) under the assumption that $\bar{b}$ is fixed. The variability in the allometry coefficient determined by the data is partitioned into 20 equal sized bins in the logarithm of the allometry coefficient. A histogram is then constructed by counting the number of data points within each of the bins as indicated by the dots in Fig. 4. The solid line segment in this figure is the best fit to these 20 numbers with minimum mean-square error. The functional form for the histogram is indicated by the curve in Fig. 4[241,242] and the quality of the fit to the diversity data is determined by the correlation coefficient $r^2 = 0.98$. The normalized histogram $G(\ln a')$ on the interval $(0, \infty)$ using the transformation

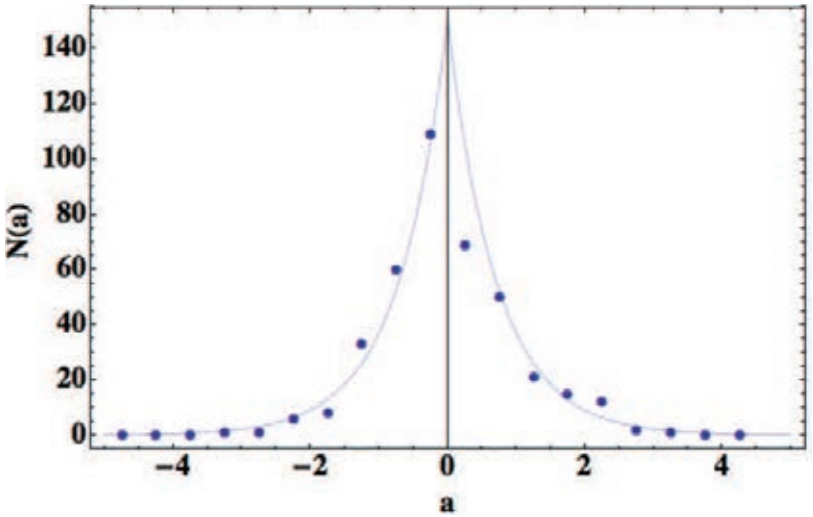

Fig. 4. The histogram of the deviations from the prediction of the AR using the data depicted in Fig. 3 partitioned into 20 equal sized bins in the logarithm of the normalized variable $a' = a/\bar{a}$. Here $\bar{a} = 0.02$ and $\bar{b} = 0.71$. The solid line segment is the best fit of Eq. (24) to the 20 histogram numbers, which yields the power-law index $\alpha = 2.79$ and the quality of the fit is measured by the correlation coefficient $r^2 = 0.98$. (Reproduced from West and West[242] with permission).

$G(\ln a')d\ln a' = P(a')da'$ gives the empirical *pdf*:

$$P(a') = \frac{\alpha}{2}\begin{cases} \dfrac{1}{a'^{1-\alpha}}\,; & a' \leq 1 \\ \dfrac{1}{a'^{1+\alpha}}\,; & a' \geq 1 \end{cases} \tag{24}$$

and $\alpha = 3.28$ yielding a standard deviation 0.017 in essentially exact agreement with the empirical data. Note that this coefficient differs from the best fit value given in the caption of Fig. 4 but this results in only a 1% change in the value of r^2.

The same inverse power-law form is obtained with $\alpha = 3.89$ and $r = 0.96$ using the avian BMR data of McNab[142] for 533 species of bird. The distribution of the deviations from the AR for both the avian and mammalian data sets fall off as inverse power laws on either side of $a = \bar{a}$. Equation (24) quantifies the qualitative argument used earlier to associate power-law *pdf*'s with multiplicative fluctuations, see also Sec. 5.

Alternatively the fluctuations can be assumed to be contained within the allometry exponent as:

$$\eta = \frac{\log(B/\bar{a})}{\log M} - \bar{b}\,. \tag{25}$$

If we assume $\bar{b} = 0.71$ and $a = \bar{a}$ then Eq. (25) provides us with the statistical fluctuations in the allometry exponent are used to construct a histogram exactly as we did previously. The solid line segment in Fig. 5 is the best fit to the 20 numbers of the histogram with minimum mean-square error. The functional form for the histogram of deviations from the allometry exponent $\bar{b}$ is determined by the curve in Fig. 5 and the quality of the fit to the histogram is determined by the correlation coefficient $r^2 = 0.97$. The histogram is fit by the Laplace *pdf*

$$\Psi(b) = \frac{\beta}{2}\exp[-\beta|b - \bar{b}|]\,, \tag{26}$$

with the empirical value $\beta = 12.85$.

3.2.1. *Co-variation of allometry coefficient and exponent*

We have obtained two separate distributions for two different parametric representations of the same data. As pointed out by Glaizer[73] species within a taxon represent a cloud of different metabolic rates and not the linear metabolic level determined by linear regression. His cloud is incorporated into the present context by abandoning the assumption that the allometry coefficient and exponent are independent and requiring that the probability of a given fluctuation is the same regardless of the representation so that $\mathcal{P}(a)da = \Psi(b)db$. In order to calculate a nonzero Jacobian of the transformation between the two allometry parameters requires that they be functionally related. West and West[243] assume $b = \bar{b} - c\ln a$, so that by inserting the

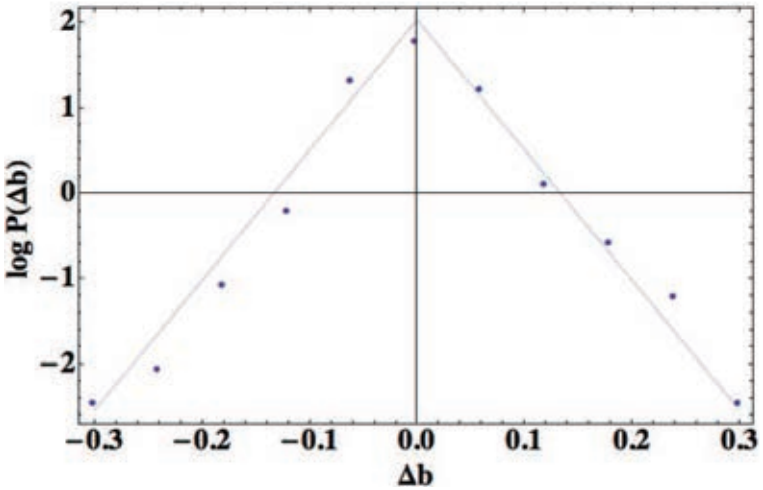

Fig. 5. The histogram of the deviations from the prediction of the AR using the allometry exponent fluctuation data partitioned into 20 equal sized bins. The solid line segment is the best fit of Eq. (26) with $\Delta b \equiv b - \bar{b}$, to the 20 histogram numbers, and the quality of the fit is measured by the correlation coefficient $r^2 = 0.97$. (Reproduced from West and West[242] with permission).

allometry exponent *pdf* Eq. (26) into that for equal probabilities and simplifying yields:

$$\mathcal{P}(a) = \frac{\beta c}{2} \begin{cases} a^{\beta c - 1} & \text{for } a \leq \bar{a} \\ \dfrac{1}{a^{\beta c + 1}} & \text{for } a \geq \bar{a} \end{cases} \tag{27}$$

and comparing Eq. (27) with Eq. (24) they identify $\alpha = \beta c$ and obtain the empirical *pdf* for the allometry coefficient $P(a')da' = \mathcal{P}(a)da$. Using the fitted values $\alpha = 2.79$ and $\beta = 12.85$ yields $c = 0.217$ and consequently the empirical transformation can be written as:

$$b = 0.71 - 0.50 \log_{10} a \,. \tag{28}$$

Note that this functional dependency of the allometry exponent on the allometry coefficient is consistent with the empirical co-variation relation obtained by Glazier[73] who used linear regression on large amounts of parametric data. West and West[243] emphasize that this co-variation of the allometry parameters implies that there is no universal value for the allometry exponent.

3.2.2. *Other scaling distributions*

The tent shaped distribution in Fig. 5 also arises using a different approach to quantifying the variability of BMR. Labra *et al.*[115] investigate BMR fluctuations by considering O_2 volume time series and examining the scaling of the high frequency fluctuations across species. They determined empirically that the standard

deviation in the BMR is proportional to the average BMR by the scaling law:

$$\mathrm{SD}_{\mathrm{BMR}} \propto B^{\lambda}$$

and $\lambda = -0.352 \pm 0.072$. This relation is known as the power curve in the ecology literature[85] and was discovered by Taylor[210] in his determination of the number of new species that can be found in a given plot of ground. It was expanded to the determination of scaling in time series by Taylor and Woiwold[211] and applied in physiology as Taylor's law in West.[238]

On the other hand Labra *et al.*[115] determined the standard deviation of BMR to be proportional to a power of the TBM:

$$\mathrm{SD}_{\mathrm{BMR}} \propto M^{\gamma}$$

and $\gamma = -0.241 \pm 0.103$. Consequently, combining the two empirical expressions for the variance we obtain:

$$B \propto M^{\gamma/\lambda} \tag{29}$$

with $\gamma/\lambda = 0.69$ a value consistent with the many fits made to the allometry data. They determine that all the species they studied show the same invariant distribution of BMR fluctuations, regardless of the difference in their phylogeny, physiology and body size. The distribution has the form Eq. (26) with the independent variable given by the fluctuation in the BMR ΔB and $\beta = \sqrt{2}/SD_{\mathrm{BMR}}$; in terms of the scaling variable $B_{\mathrm{sc}} \equiv \sqrt{2}\Delta B/\mathrm{SD}_{\mathrm{BMR}}$ curves for 12 different species collapse onto a single universal curve.

3.2.3. *Paleobiology and scaling*

Phenomena with intermittent properties described by inverse power-law statistics are apprarently ubiquitous[233] and paleobiology is no exception. Bak and Boettcher[8] interpreted Charles Lyell's[125] uniformitarianism as meaning that all geologic activity should be explainable in terms of readily available processes working at all times and all places with the same intensity. They go on to argue that the existence of earthquakes, volcanic eruptions, floods and tsunamis all indicate that the physical world is not in equilibrium. Moreover the intermittent nature of the paleontological record indicates that macroevolution is also out of equilibrium and consequently the inverse power-law statistics are possibley suitable for their description.

Eldredge and Gould[52] argued that punctuated change dominates the history of life and that relatively rapid episodes of speciation constitute biological macroevolution. The intermittency of speciation in time has been explained by one group as *punctuated equilibria*[51] and has been indirectly related to fractal statistics by identifying it as a self-organized critical phenomenon.[8] In the self-organized criticality model of speciation Bak and Boettcher[8] associate an avalanche of activity with exceeding a threshold and the distribution of returns to the threshold with a "devil's staircase" having a distribution of steps of stasis of lengths given by the

inverse power-law *pdf*, that is, $T^{-\gamma}$ with $\gamma = 1.75$. Moreover, as explained by Sneppen *et al.*,[206] the number of genera N, with a lifetime T can be fitted very well to a power law $T^{-\beta}$ with $\beta \approx 2$.[173] More recently Rikvold and Zia[179] put forward an explanation of punctuated equilibrium based on $1/f$ noise in macroevolutionary dynamics that also yields an inverse power-law *pdf* for the life time of ecological communities with $\beta = 2$.

Solé *et al.*[208] analyzed the statistics of the extinction fossil record (time series) and determined that the power spectrum has the form:

$$S(f) \propto 1/f^{\mu}\,,$$

with $0 < \mu < 2$. They find $0.80 \leq \mu \leq 0.90$ and argue that these values support the self-organized criticality interpretation of extinction. On the other hand, Plotnick and Sepkowski[165] also find a $1/f$ power spectrum with a power-law index for extinction consistent with Solé *et al.*[208] and indices for species generation of approximately half that for extinction. However the latter authors conclude that their results are incompatible with self-organized criticality and instead are compatible with multifractal self-similarity in both the extinction and generation records.

4. Models of Allometry

Two distinct methods dominate the many derivations of AR. One method is based on the first-principles reductionistic approach starting from an assumed form for the underlying mechanisms and from that deducing the necessity of Eq. (2). The other method is phenomenological involving statistical analysis and identifying patterns in the data analysis and from these patterns deducing the necessity of the empirical AR. A number of the statistical methods were reviewed in the previous section. The ARs stand out as empirical relations that have withstood the test of time, whereas the same cannot be said for the models developed to explain how they come about. In this section we examine attempts to formulate general principles from which the underlying mechanisms, whether reductionist or statistical, producing the ARs can be identified.

The search for an *unifying principle* parallels such historical activities as the determination of "least action" in analytic mechanics or optimization in control theory. More recently investigators have rediscovered Newton's "principle of similitude"' introduced in the *Principia* (II, Proposition 32). Scaling and the principle of similitude have been present in the study of complex physical phenomena since physics became a science. In modern times it is RG theory that provides a formalism for determining how force is transferred across multiple scale.[103,111,259] Part of the reason for exploring this approach is that fractal geometry and fractal statistics are able to capture some of the regularity observed in vast amounts of data in the life and social sciences in addition to the physical sciences. The implementation of fractal geometry and RG theory to study the architecture of physiological forms,[17,228,247] interacting networks of chemical reactions[45,78,169] and

the topology of ecological webs[27] over the past quarter century has lead to some remarkable insights. In particular the descriptive success of investigations using fractals[15,131,135,143] suggests that branching networks with fractal architectures have an evolutionary advantage[230,231,235] as do fractal stochastic processes.[236]

4.1. *Optimization principles*

Optimization provides one of the best recipes for determining network dynamics consistent with a given set of constraints. It is through the specification of the constraints that insight into a phenomenon is introduced. The biological sciences employ ideas such as energy minimization; the minimal use of materials along with the maximization of efficiency. So whether the extremum is a minimum or maximum depends on one's purpose and the quantity being varied.

4.1.1. *Energy minimization*

Scaling relations in living networks result from the balancing of various constraints. One such biological balancing is that of energy utilization against the energy cost of carrying out a biological function. A technique that has been used both implicitly and explicitly in the derivation of ARs is supplying nutrients to various parts of an organism through the venous and capillary networks as well as through the respiratory network. Murray[150] considered a fluid with viscosity ν and laminar flow Q within a tube of length l and radius r. The flow had to overcome the vascular resistance that generates a pressure difference along the length of the tube given by Poiseuille's law $\Delta p = 8l\nu Q/\pi r^4$.

A constraint on the flow is the cost of transporting fluid of cylindrical volume $V = \pi l r^2$ along the tube so that introducing c as the cost factor the total work to be done per unit time is given by:

$$E = Q\Delta p + cV = \frac{8l\nu Q^2}{\pi r^4} + c\pi l r^2 \,. \tag{30}$$

Consequently, minimizing this expression with respect to the radius yields the optimal flow: $Q = Cr^3$ with the constant $C = \sqrt{c\pi^2/16\nu}$. The cubic dependence of the flow rate on radius is known as Murray's law[223] and is indicative of the maximum efficiency of the flow.

Murray[151] subsequently extended his result to bifurcating networks such as occurs in bronchial airways. The flow from a parent vessel of radius r_0 branches into two daughter vessels r_1 and r_2 such that the flow divides:

$$Q_0 = Q_1 + Q_2 \,.$$

Therefore inserting Murray's law into this expression yields da Vinci's equation with $\alpha = 3$ and in the case of equal radii in the daughter branches $r_1 = r_2$ we obtain the scaling relation $r_1 = 2^{-1/3} r_0$. Thus, the maximally efficient bifurcating network in terms of energy transport cost has radii decreasing as the cube root of two. As

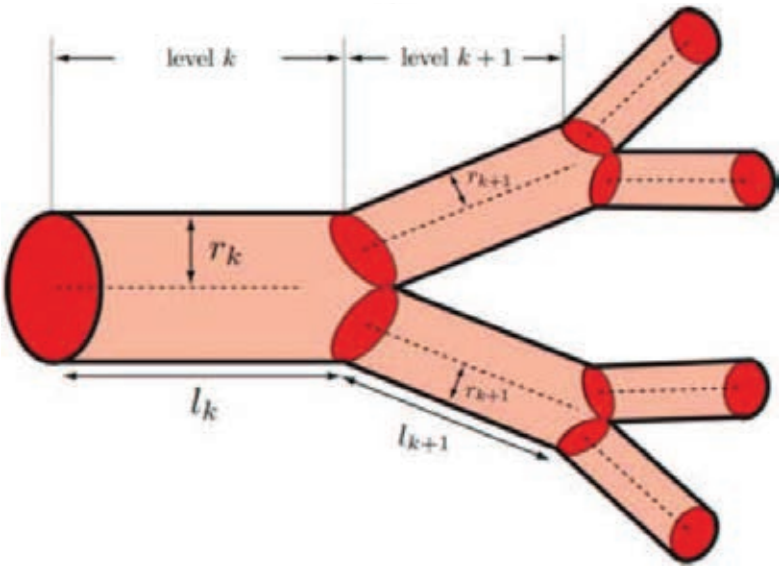

Fig. 6. Sketch of a branching structure such as a blood vessel or bronchial airway with the parameters used in a bifrucating network model.

pointed out by Weibel[223] this last result is also known as Murray's law. However this law was actually first formulated by Hess[89] for blood vessels and subsequently is more properly called the Hess–Murray law.

4.1.2. *Optimal design*

Rashevsky[172] introduced the *principle of optimal design* in which the material used and the energy expended to achieve a prescribed function is minimal. He applied the principle to the basic problem of how the arterial network could branch in space in order to supply blood to every element of tissue. To address this problem he used the model of a bifurcating branching network supplying blood to a restricted volume and reducing the total resistance to the flow of blood. His purpose was to determine the condition imposed by the requirement that the total resistance is minimum.

Here we assume the branching network is composed of N generations from the point of entry (0) to the terminal branches (N). A typical tube at some intermediate generation k has length l_k, radius r_k and pressure drop across the length of the branch Δp_k as sketched in Fig. 6. The volume flow rate Q_k is expressed in terms of the flow velocity averaged over the cross sectional area $u_k : Q_k = \pi r_k^2 u_k$. Each tube branches into n smaller tubes with the branching of the vessel occurring over some distance that is substantially smaller than the lengths of the tubes of either generation. Consequently, the total number of branches generated up to generation k is $N_k = n^k$. The pressure difference at generation k between the ends of a tube

is given by a suitably indexed version of Poiseuille's law and the total resistance to the flow is given by the ratio of the pressure to flow rate

$$\Omega_k = \frac{\Delta p_k}{Q_k} = \frac{8\nu l_k}{\pi r_k^4}\,. \tag{31}$$

The total resistance for a network branch with m identical tubes in parallel is $1/m$ the resistance of each individual tube. Thus, in this oversimplified case we can write the total network resistance as:

$$\Omega_T = \frac{8\nu l_1}{\pi r_0^4} + \frac{8\nu}{\pi}\sum_{j=1}^{N}\frac{1}{N_j}\frac{l_k}{r_j^4}\,. \tag{32}$$

In order to minimize the resistance for a given mass Rachevsky first expressed the initial radius r_0 in terms of the total mass of the network. The optimum radii for the different branches of the bifurcation network having the total mass M are then determined such that the total resistance is a minimum $\partial\Omega_T/\partial r_j = 0$ yielding the equality $r_k = N_k^{-1/3} r_0$. The ratio of the radii between successive generations is $r_{k+1}/r_k = (N_k/N_{k+1})^{1/3}$so that inserting the number of branches at the kth generation $N_k = n^k$ yields:

$$r_{k+1}/r_k = n^{-1/3}\,, \tag{33}$$

yielding an exponential reduction in the branch radii across generations. Note the formal similarity of this ratio to Horton's law in which the ratio of numbers of river branches is independent of generation number.

Rashevsky considered the bifurcating case $n = 2$ where the ratio of radii reduces to $r_{k+1}/r_k = 2^{-1/3} = 0.794$. This is the classic "cube law" branching of Thompson[213] in which he used the "principle of similitude". The value $2^{-1/3}$ was obtained by Weibel and Gomez[222] for the reduction in the diameter of bronchial airways for the first ten generations of the bronchial tree. However they noted a sharp deviation away from this constant fractional reduction after the tenth generation. The value $2^{-1/3}$ was also obtained by Wilson[260] who explained the proposed exponential decrease in the average radius of a bronchial tube with generation number by showing that this is the functional form for which a gas of given composition can be provided to the alveoli with minimum metabolism or entropy production in the respiratory musculature. He proposed minimum entropy production[69] as the design principle for biological networks to carry out a given function.

The deviation from classical (exponential) scaling above generation ten shown in Fig. 7 was eventually explained using an alternative model of the bronchial airways in terms of fractal statistics[228] as we subsequently discuss.

4.2. *Metabolic allometry*

Barenblatt and Monin[14] proposed that metabolic scaling might be a consequence of the fractal nature of biology, but they did not provide a mechanistic model for its

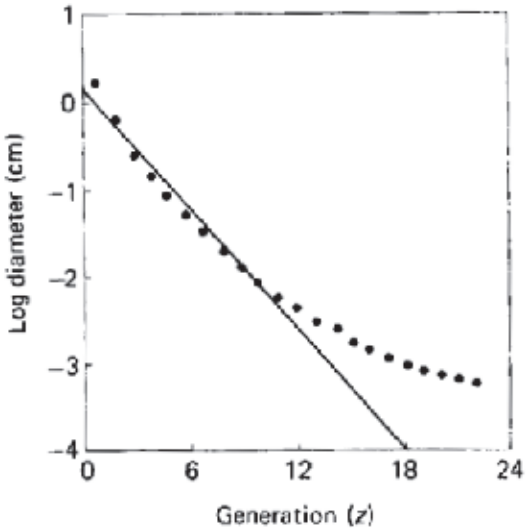

Fig. 7. As the bronchial tree branches out, its tubes on average decrease in size. A theory consistent with the Principle of Similitude[213] predicts that their diameters should decrease by about the same ratio from one generation to the next; exponential decline. This semilog graph shows measurements from Weibel and Gomez[222] for 23 generations of bronchial tubes in the human lung. The prediction is a straight line that fits the anatomic data (dots) until about the tenth generation, after which they deviate systematically from an exponential decline. [adapted from West and Goldberger.[229]]

description. This shortcoming has been overcome by a number of investigators who have devised numerous fractal models to describe AR in a variety of contexts.[228,247]

4.2.1. *Elastic similarity model*

The first model to analytically predict the allometry exponent 3/4 was constructed by McMahon.[139,140] His argument rests on the observation that the weight of a column increases more rapidly with size than does its strength. Moreover as discussed by Schmidt–Nielsen[195] if the column is tall and slender it can fail due to elastic buckling in which small lateral displacements exceed the elastic restoring forces. For a sufficiently slender column with Young's elastic modulus E and density ρ the critical length of a column of diameter d is:

$$l_{\rm cr} = k(E/\rho)^{1/3} d^{2/3} \tag{34}$$

and k is a constant. The elastic criteria of McMahon is therefore given by $l^3 \propto d^2$. The weight of the column is given by the product of the density, length and cross-sectional area,

$$Mg = \rho d^{2/3} \pi d^2/4\,,$$

where the length has been replaced using the elastic criteria yielding $d \propto M^{3/8}$.

The implications for allometry of the scaling between cylinder diameter and mass was discussed by Calder[31] using the symmorphosis hypothesis of Taylor and Weibel:[212] "... is regulated to satisfy but not exceed the requirements of the functional system".[237] First off we recognize that locomotion requires the contraction of muscles. During contraction, muscles exert a force that increases with the cross-sectional area of the muscle. The power output of the muscle is the work done per unit time and may be equated with the metabolic rate, the product of the force generated by the muscle and the velocity u of the shortening of the muscle $B \propto d^2u$. The velocity of the shortening of the muscle appears to be a size-independent constant from species to species[92] so that using these two equations for the diameter yields:

$$B \propto M^{3/4}\,.$$

Consequently, the allometry exponent 3/4 in McMahon's elastic similarity model is required to maintain the flow of energy to the working muscles and is consistent with the principle of symmorphosis.

Versions of the above argument given by both Calder[31] and Schmidt–Nielsen[195] seem to explain the value of the allometry exponent for warm blooded animals. Dodds *et al.*[47] critique McMahon's model by noting that there is no compelling reason why the power output of muscles should be the dominant factor in the scaling of BMR. Moreover, Savage *et al.*[189] point out that while the elastic similarity model might apply to the bones of mammals or the trunks of trees that have adapted to gravitational forces, it is doubtful that it is applicable to aquatic or unicellular organisms that also display an allometry exponent of 3/4.[87]

4.2.2. *WBE model*

West, Brown and Enquist[247] (WBE) published a quantitative model of metabolic AR that has had significant impact on how a significant fraction of today's biology/ecology community understands metabolic ARs. WBE model nutrient distribution within a hierarchal network in which vessels become narrower, shorter and more numerous between successive levels proceeding from the initial to the terminal level reminiscent of representations of river branchings. The scaling in the transport network is a consequence of the constraints imposed by three assumptions: (1) The entire volume of the organism is crammed with a space-filling branching network. (2) The tube properties at the terminus of the network are size-invariant. (3) The energy required to distribute resources using this network is minimal, that is, the hydrodynamic resistance of the network is minimized. We note their claim that this model is the origin of universal scaling laws in biology[248,249] with $b = 3/4$. However we recall at the start that the existence of an empirical exponent $b = 3/4$ for metabolic AR has been questioned by numerous investigators[47,91,113,114,128] and we address these concerns and others in due course.

WBE introduce two parameters to characterize the network branching process, $\beta_k = r_{k+1}/r_k$ the ratio of successive branch radii, as was done in the energy minimization arguments[172] and the other is $\gamma_k = l_{k+1}/l_k$, the ratio of successive branch lengths. They conclude that the total number of terminal branches scales with TBM as $N_T = (M/M_0)^b$. The total number of branches at level k is $N_k = n^k$. Consequently at the network terminus the self-similarity of the network yields $N_T = n^N$ and consequently the total number of branches is:

$$N = b \ln(M/M_0)/\ln n\,. \tag{35}$$

Rashevsky's energy minimization argument indicates that the transport of nutrients in complex networks is maximally efficient when β_k is independent of k. This is the "fractal" scaling assumption made by WBE.

The estimates of the ratio parameters required two separate assumptions. To estimate the ratio of lengths WBE assume that the volume of a tube at generation k can be replaced by a spherical volume of diameter l_k and in this way implement the space-filling assumption. The conservation of volume between generations therefore leads to the space filling condition:

$$(l_{k+1}/l_k)^3 \approx N_k/N_{k+1} = n^{-1}$$

and consequently to the k-independent parameter

$$\gamma = \gamma_k = n^{-1/3}\,.$$

They maintain that this level-independent scaling of the lengths is a generic property of all the space-filling networks they consider. This condition for an n-branching network with a reduction in size of $n^{-1/3}$ between successive generations yields using the definition for the fractal dimension $D = \log n/\log n^{1/3} = 3$.

A separate and distinct assumption is made to estimate β using the classic rigid-pipe model to equate the cross-sectional areas between successive generations: $\pi r_j^2 = n\pi r_{j+1}^2$, so that we have

$$\beta = \beta_k = n^{-1/2}\,.$$

Note that this scaling of β differs from the ratio parameter obtained using energy minimization. Inserting these values of the scaling parameters into the expression for b yields the sought after exponent $b = 3/4$. This value of the exponent in turn determines a number of other quarter-power scaling laws.

WBE point out that this is strictly a geometrical argument applying only to those networks that exhibit area-preserving branching. Moreover the fluid velocity is constant throughout the network and it is independent of size. They go on to say that these features are a natural consequence of the idealized vessel-bundle structure of plant vascular networks in which area-preserving arises automatically because each branch is assumed to be a bundle of n^{N-k} elementary vessels of the same radius. They recognized that this is not the situation with vascular blood flow where the beating of the heart produces a pulsating flow that generates a very

different kind of scaling. Area-preserving is also not true in the mammalian lung where there is a distribution of radii at each level of branching.

A physical property that the area preserving condition violates is that blood slows down in going from the aorta to the capillary bed. Here WBE return to the principle of energy minimization and as stated by West[248] assert that to sustain a given metabolic rate in an organism of fixed mass, with a given volume of blood, the cardiac output is minimized subject to a space-filling geometry. This variation is essentially equivalent to minimizing the total impedance since the flow rate is constant and again yields the Hess–Murray law $\beta = n^{-1/3}$ corresponding to area-increasing branching.[6,190] This change in scaling from the area-preserving $n^{-1/2}$ to the area-increasing $n^{-1/3}$ solves the problem of slowing down blood flow to accommodate diffusion at the capillary level. Moreover, the variation also leads to an allometry exponent $b = 1$. Such an isometric scaling ($b = 1$) suggests that plants and animals follow different allometry scaling relations as was found.[174,201]

A detailed treatment of pulsate flow is not straightforward and will not be presented here, but see Savage *et al.*[190]; Silva *et al.*[201] and Apol *et al.*[6] for details and commentary in the context of the WBE model. We do note that for blood flow the walls of the tubes are elastic and consequently the impedance is complex, as is the dispersion relation that determines the velocity of the wave and its frequency. Consequently pulsate flow is attenuated[32,60] and WBE argue that the impedance changes its r-dependence from r^{-4} for large tubes to r^{-2} for small tubes. The variation therefore changes from area-preserving flow $\beta = n^{-1/2}$ for large vessels to dissipative flow $\beta = n^{-1/3}$ for small vessels where blood flow is forced to slow. Thus β_k is k-dependent in the WBE model for pulsate flow and at an intermediate value of k the scaling changes and this changeover value is species dependent. These results are contradicted in the more extensive analysis of pulsate flow by Apol *et al.*,[6] who conclude that Kleiber's law remains theoretically unexplained.

Kozlowski and Konarzewski[113] critique the apparent limitations of the WBE model assumptions. The size-invariance assumption has been interpreted by them to mean that $N_T \propto M$, that is, the terminal number of vessels scales isometrically with size and consequently causes the number of levels to be a function of body size since more levels are required to fill a larger volume with the same density of final vessels. However Brown *et al.*[28] assert that $N_T V_T \propto M$ so that

$$N_T \propto M^{3/4} \tag{36}$$

to which Kozlowski and Konarzewski[114] respond that such mass dependence is an arbitrary assumption and is not proven, see also Dawson.[43] Etienne *et al.*[54] reconstruct the WBE model without making the self-similarity assumption and in so doing satisfy the concerns of Kozlowski and Konarzewske.[113,114] The arguments remain unresolved and Cyr and Walker[38] refer to the assumption embodied in Eq. (36) as the illusion of mechanistic understanding and maintain that after a century of work the jury is still out on the magnitude of the allometry exponents. Riisgård[180] argues that respiration and growth are integrated through the energetic

costs of growth and that this explains why the b value is not a "natural constant" and that a "3/4 power scaling law cannot be deduced from the interplay between pure physical and geometric constraints of the transport of oxygen.

A quite different critique comes from Savage *et al.*[190] who emphasize that the WBE model is only valid in the limit $N \to \infty$, that is, for infinite network size (body mass) and that the actual allometry exponent predicted depends on the sizes of the organisms considered. They calculate that the AR between BMR and TBM have corrections for finite N given by:

$$M = a_1 B + a_2 B^{4/3} \tag{37}$$

from which it is clear that $b = 3/4$ only occurs when $a_2 B^{1/3} \gg a_1$. This inequality is not satisfied for bodies of finite size. In their original publication WBE acknowledged the potential importance of such finite-size effects, especially for small animals, but the magnitude of the effect remained unspecified. Using explicit expressions for the coefficients in the WBE model Savage *et al.*[190] show that when accounting for these corrections over a size range spanning the eight orders of magnitude observed in mammals a scaling exponent of $b = 0.81$ is obtained. Moreover in addition to this strong deviation from the desired value of 3/4 there is a curvilinear relation between the TBM and the BMR in the WBE model given by:

$$\ln M = \ln a_2 + \frac{4}{3} \ln B + \ln \left(1 + \frac{a_1}{a_2} B^{-1/3} \right),$$

whose curvature is opposite to that observed in the data. Consequently they conclude that the WBE model needs to be amended and/or the data analysis needs reassessment to resolve this discrepancy. A start in this direction has been made by Kolokotrones *et al.*[110] Agutter and Tuszynski[5] also review the evidence that the fractal network theory for the two-variable AR is invalid.

Another variation on this theme was made by Price *et al.*[168] who relax the fractal scaling assumptions of WBE and show that allometry exponents are highly constrained and covary according to specific quantitative functions. Their results emphasize the importance of network geometry in determining the allometry exponents and supports the hypothesis that natural selection minimizes hydrodynamic resistance. Moreover they extended McMahon's elastic similarity model and apply it to plant scaling exponents showing its consistency with their modification of WBE.

Prior to WBE there was no unified theoretical explanation of quarter-power scaling. Banavar *et al.*[12] show that the 3/4 exponent emerges naturally as an upper bound for the scaling of metabolic rate in the radial explosion network and in the hierarchical branching networks models and they point out that quarter-power scaling can arise even when the underlying network is not fractal.

Finally, Weibel[224] presents a simple and compelling argument on the limitations of the WBE model in terms of transitioning from BMR to the maximal metabolic rate (MMR) induced by exercise. The AR for MMR has an exponent $b = 0.86$

rather than 3/4, so that a different approach to determining the exponent is needed. Painter[158] demonstrates that the empirical allometry exponent for MMR can be obtained in the manner pioneered by WBE by using the Hess–Murray law for the scaling of branch sizes between levels.

Weibel[224] argues that a single cause for the power function arising from a fractal network is not as reasonable as a model involving multiple causes, see also Agutter and Tuszynski.[5] Darveau *et al.*[41] propose such a model recognizing that the metabolic rate is a complex property resulting from a combination of functions. West *et al.*[251] and Banavar *et al.*[11] demonstrate that the mathematics in the distributed control model of Darveau *et al.*[41] is fundamentally flawed. In their reply Darveau *et al.*[42] do not contest the mathematical criticism and instead point out consistency of the multiple-cause model of metabolic scaling with what is known from biochemical[205] and physiological[101] analysis of metabolic control. The notion of distributed control remains an attractive alternative to the single cause models of metabolic AR. A mathematically rigorous development of AR with fractal responses from multiple causes was recently given by Vlad *et al.*[218] in a general context. This latter approach may answer the formal questions posed by many of these critics.

4.3. *Why fractal transport?*

Why are fractals important in the design of allometry networks? Barenblatt and Monin[14] suggested that metabolic scaling might be a consequence of the fractal nature of biology and WBE determined that fractal geometry maximizes the efficiency of nutrient transport in biological networks. Weibel[223] maintains that the fractal design principle can be observed in all manner of physiologic networks quantifying the observations and speculations of Mandelbrot,[131,132] as does West.[238]

West[230] conjectured that fractals are more adaptive to internal changes and to changes in the environment than are classical processes and structures. Consider a network property characterized by classical scaling at the level k such as the length or diameter of a branch $F_k \propto e^{-\lambda k}$ compared with a fractal scaling characterization of the same property $F_k \propto k^{-\lambda}$. What is significant in these two functional forms for the present argument is the dependence on the parameter λ. The exponential has emerged from a large number of optimization arguments and the inverse power-law results from RG scaling arguments.

Assume the parameter λ is the sum of a constant part λ_0 and a random part ξ. The random part can arise from unpredictable changes in the environment during morphogenesis, non-systematic errors in the code generating the physiologic structure or any of a number of other causes of irregularity. Thus, regardless of whether the errors are induced internally or externally, the average is taken over an ensemble of zero-centered Gaussian fluctuations ξ with variance $\sigma^2/2$. Note that the choice of Gauss statistics has no special significance here except to provide closed form expressions for the averages to facilitate discussion. The relative error generated by

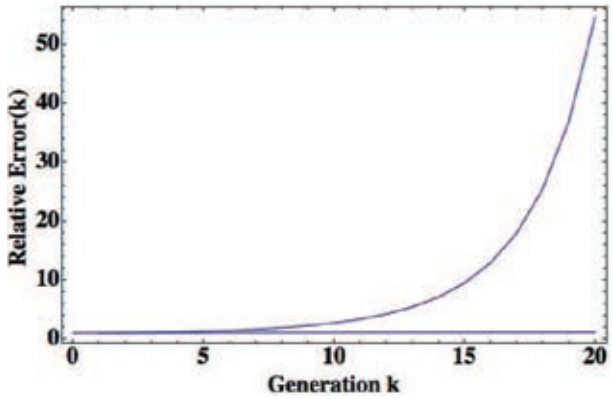

Fig. 8. The error between the model prediction and the prediction averaged over a noisy parameter is shown for the classical model (upper curve) and the fractal model (lower curve).

the fluctuations is given by the ratio of the average value to the function in the absence of fluctuations, yielding the relative error for classical scaling $\varepsilon_k = \exp[\sigma^2 k^2]$ and for fractal scaling $\varepsilon_k = \exp[\sigma^2 (\ln k)^2]$.

The two error functions are graphed in Fig. 8 for fluctuations with a variance $\sigma^2 = 0.01$. At $k = 15$ the error in classical scaling is 9.5. This enormous relative error means that the perturbed average property at generation 15 differs by nearly an order of magnitude from what it would be in an unperturbed network. A biological network with this sensitivity to error would not survive for very long in the wild. For example, the diameter of a bronchial airway in the human lung could not survive this level of sensitivity. However, the property of the fractal network only changes by 10% at the distal point $k = 20$. The implication is that the fractal network is relatively unresponsive to fluctuations.

A fractal network is consequently very tolerant of variability. This error tolerance can be traced back to the broadband nature of the distribution in scale sizes of a fractal object. This distribution ascribes many scales to each generation in the network. The scales introduced by the errors are therefore already present in a fractal object. Thus, the fractal network is *preadapted* to variation and is therefore insensitive to change.[230,231] These conclusions do not vary with modification in the assumed statistics of the errors. Therefore let us review how fractal statistics have been employed in the understanding of some nonmetabolic physiologic ARs.

4.3.1. *WBG bronchial tree*

The energy minimization argument applied to a branching network resulted in Horton's law. However, the theoretical arguments justifying this empirical law and others like it assume that the network is geometrically self-similar. Real networks, such as the bronchial tree in the mammalian lung, do not have such deterministic regularity. At any generation of the bronchial airway there is a distribution of

lengths and diameters, with a reduction in the average length and average diameter between successive generations. Consequently, the simple characteristic scale governing the decrease in bronchial dimensions across generations given by the Hess–Murray law must be reexamined. West, Barghava and Goldberger[228] (WBG) assumed the mammalian lung to be a fractal structure having a distribution of scales contributing to the variability in tube size at each generation. This model yields an average bronchial diameter that decreases with generation number, not as an exponential as suggested by Weibel and Gomez,[222] but as an inverse power law.[229,232,233]

WBG assume that the variability in the diameters of the bronchial tubes at generation k is given by $d(\gamma k)$, where γ is a random variable that determines the size of the diameter. In the energy minimization argument we determined that $\gamma = \ln 2/3$ and the classical reduction in diameter with generation number was exponential $d(\gamma k) = d_0 e^{-\gamma k}$ as shown in Fig. 7. However with real data this is the reduction in the average diameter just as it was for other allometry networks so that the random variation in diameter at generation k is smoothed over to determine the average. Formally the behavior of the average diameter as a function of generation number is given by:

$$\overline{d(k)} = \int d(\gamma k) p(\gamma) d\gamma \,, \tag{38}$$

with $p(\gamma)$ the *pdf* in scale size. Rather than prescribe a particular functional form to this *pdf* in the formal definition WBG use a RG argument originally developed in an economic context by Montroll and Shlesinger.[148] Assuming the original distribution of scales has an average value $\bar{\gamma}$ the RG argument constructs a new distribution with an infinite number of new scales each a factor of β larger than the preceding scale and each occurring with a relative frequency ζ less often. The distribution resulting from the RG relation gives rise to an empirical average denoted by brackets in terms of the formal average Eq. (38) as follows[234,235]:

$$\langle d(k) \rangle = \zeta \langle d(\beta k) \rangle + (1 - \zeta) \overline{d(k)} \,. \tag{39}$$

The dominant behavior for the solution to the RG relation Eq. (39) is determined by the singular part of the solution to the equation, which for simplicity WBG write with a subscript $\langle d(k) \rangle_s = \zeta \langle d(\beta k) \rangle_s$. Shlesinger and West[200] note that the solution to this scaling equation that provides the best fit to the data can be written as the real part of:

$$\langle d(k) \rangle_s = \sum_{n=-\infty}^{\infty} \frac{\mathcal{A}_n}{k^{\mu_n}} \,; \quad \mu_n = b + i 2\pi n / \ln \beta \,; \tag{40}$$

μ_n is the complex fractal dimension of order n for the branching process, with the exponent $b = -\ln \zeta / \ln \beta > 0$ and the $\mathcal{A}_n$ are fit by experimental data. Of course there is in addition to Eq. (40) an analytic part to the solution that WBG calculated but which becomes negligible with increasing k.

Thus, the average diameter is an inverse power law in the generation number modulated by a slowly oscillating function just as observed in the data depicted in Fig. 9. This fractal model of the bronchial airway provides an excellent fit to the average bronchial tube diameter data in four distinct species: dogs, rats, hamsters

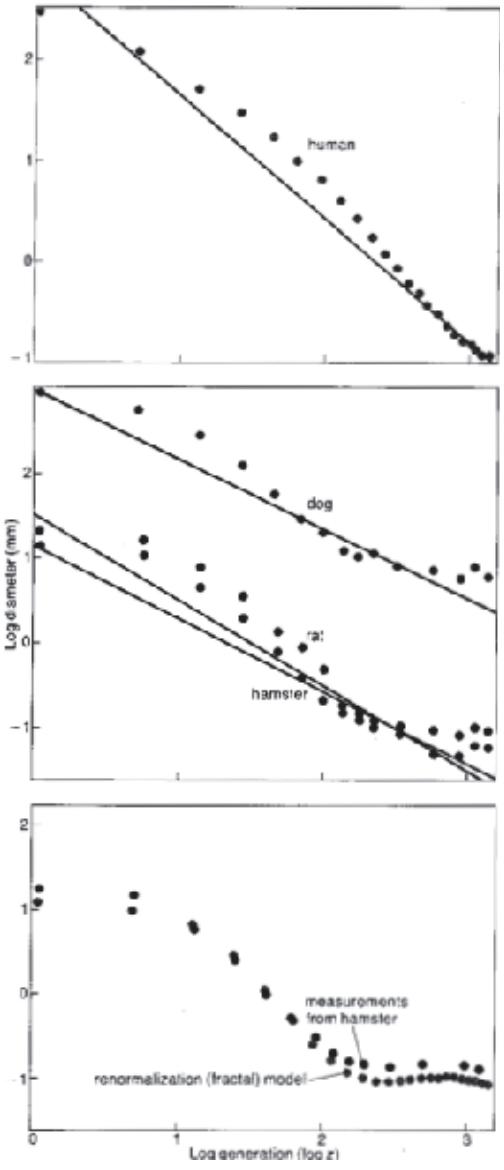

Fig. 9. Top: Reploted data from Fig. 7 on log–log scales for humans. Center: The harmonic variation in measurements for dogs, rats and hamsters taken by Raabe *et al.* (1976). Bottom: The average diameters for the bronchial tubes of a hamster and RG (fractal) model prediction using Eq. (40). [Adapted from West and Goldberger[228]].

and humans.[152] The quality of the fit is shown for hamsters in Fig. 9, which restricts the summation index in Eq. (40) to $n = 0, 1, -1$ and $\mathcal{A}_1 = \mathcal{A}_{-1}$ yields a single oscillation of the modulation function fit to the data.

The form of Eq. (40) strongly suggests that the RG relation for the average diameter captures a fundamental property of the structure of the lung that is distinct from classical scaling. There is an AR at each level of the bronchial tree with the average diameter decreasing as k^{-b} with the level being a measure of size. Moreover the data show the same type of scaling for bronchial tube lengths and consequently volume.

4.3.2. *Distribution of bronchial diameters*

Kitaoka and Suki[107] use a related but distinct analysis of the lung data depicted in Fig. 9 in which they investigate the statistical variability of the bronchial airway diameters. Their analysis was based on the assumed relation between the airflow rate and the airway diameter d:

$$Q = Cd^{\alpha}\,,$$

a relation discussed in terms of energy optimization by Murry[150] yielding $\alpha = 3$. The relation was also considered in a bronchial airway context by a number of other investigators.[82,105,163] The data of Raabe *et al.*[171] reveals that the flow rate is a random variable and that the cumulative probability for the flow rate to exceed Q is given by:

$$\Pr(\geq Q) \propto 1/Q$$

with an inverse power-law index of -1 to three significant figures. Note that from the additive form of the flow rate between successive generations and the da Vinci relation between parent and daughter branches that the *pdf* for the diameter of the bronchial airway is determined to be:

$$p(d) = Cd^{-(\alpha+1)}\,, \quad C = \frac{\alpha(d_0 d_T)^{\alpha}}{d_0^{\alpha} - d_T^{\alpha}} \tag{41}$$

with d_0 the diameter of the thorax and d_T the diameter of the smallest bronchial airway. Here again the empirical distribution for the observable, the bronchial tube diameter rather than the allometry coefficient, is an inverse power-law (Pareto) *pdf*.

Note that in the previous subsection the average diameter was expressed as an inverse power law in the generation number. The distribution in the size of the bronchial airway Eq. (41) does not directly depend on generation number and is an inverse power law in diameter size, that is, in millimeters as depicted in Fig. 10. The data used to construct Fig. 9 was also used to determine the cumulative distribution of airway diameters and yields the inverse power-law distribution with $\alpha = 3.1$ with correlation coefficient of $r^2 = 0.988$. Note that this value of the exponent is slightly different from the optimum as we discuss in the next section. It is also noteworthy that the oscillations around the inverse power law given by the straight line are the

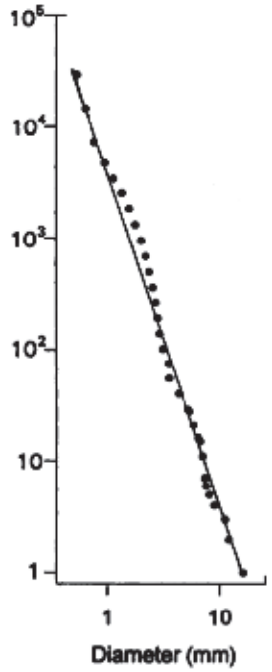

Fig. 10. Cumulative distribution of diameters on log–log plot. The regression model over the full range of diameters yields $\alpha = 3.1$ with $r^2 = 0.988$. [Reproduced from Kitaoka and Suki[107] with permission].

same periodic variation explained using WBG theory except that the oscillations are now a function of distance rather than generation number.

4.3.3. *The optimum can be dangerous*

A question of interest is whether optimal design criteria are ever realized in nature and whether they are even desirable. The WBE model suggests that the allometry exponent value of 3/4 is proof of the optimally of fractal design of networks for nutrient transport. However the controversy over the empirical value of the allometry exponent calls this implication into question. The present discussion regarding the mammalian lung and whether the bronchial tree is optimal has been investigated by Mauroy *et al.*[138] They maintain that the bronchial tree of most mammalian lungs is a good example of an efficient distribution network with an approximate fractal structure.[152,228] They state that physical optimization is critical in that small variations in the geometry can induce large variations in the net air flux and consequently optimality cannot be a sufficient criterion for physiologic design of the bronchial tree. The slight deviations observed in the parameters presumed to be optimized are a manifestation of a safety factor being encorporated into the design and into the capacity for regulating airway caliber.

In the present context the size ratio h of successive airway segments are homothetic with $h = 2^{-1/3} \approx 0.79$ as discussed earlier. Homothetic scaling means that the lengths and diameters have the same ratios between successive generations. Using the resistance minimization argument for the bronchial network Mauroy *et al.*[138] show that the "best" bronchial tree is fractal with constant reduction factor given by the Hess–Murray law. Do the data support this optimal value and if not what does that imply about the efficiency of bronchial airways?

The fractal dimension for a bronchial airway is $D = -\ln 2/\ln h$ so that the Hess–Murray law implies $D = 3$ whereas $h > 0.79$ implies $D > 3$. In the human lung it is found that the homothety ratio is $h \approx 0.85$[224] and the bronchial network is therefore not optimized: its volume is too large and its overall resistance is too small. Mauroy *et al.*[138] emphasize that this deviation from optimal is, in fact, a safety margin for breathing with respect to possible bronchial constrictions.

Sapoval[187] has argued that without regulation of the airway caliber[170] there would be a multifractal spatial distribution of air within the lungs, resulting in strongly nonuniform ventilation with some regions of the lung being poorly fed with fresh air. Expanding on this theme using inhomogeneity of the homothety ratio Mauroy *et al.*[138] show how the optimal network is dangerously sensitive to physiological variability and consequently design of the bronchial tree must incorporate more than just physical optimality. This argument has clear implications for other allometric networks.

5. Probability Calculus and ARs

A fractal processes is one that is rich in scales with no one scale being dominant. Thus, information in fractal phenomena is coupled across multiple scales manifesting long-time memory, as for example, observed in the architecture of the mammalian lung,[152,223,228] manifest in the long-range correlations in human gait[84,235] and measured in the human cardiovascular network,[161] all of which are discussed in West.[238] These phenomenological characterizations of fractal time series relate back to the observation made earlier that if $X(t)$ and $Y(t)$ are stochastic time series then $Y(X)$ must be a random function of its random argument as well. Consequently the general approach to determining the relation between such variables is through their *pdf*'s.

In this section we examine *pdf*'s that can produce the interspecies metabolic ARs as a relation between moments. To do this requires a brief review of some methods from nonequilibrium statistical physics[118,175] and their extension to fractional equations of motions.[108,236]

5.1. *Stochastic differential and Fokker–Planck equations*

There are two major techniques available in statistical physics for the modeling of stochastic phenomena. The first technique uses the dynamic equations constructed by Langevin[117] who introduced uncertainty through a random force in the equations

of motion. The second technique is based on the phase space evolution of the *pdf* using the Fokker–Planck equation (FPE). The conditions under which these two methods are equivalent have been shown in a number of places, see, for example, Lindenberg and West.[118]

5.1.1. *Additive fluctuations*

Consider the dynamics of a simple exponential relaxation process $Z(t)$ that is disrupted by a random force $\xi(t)$:

$$\frac{dZ(t)}{dt} = -\lambda Z(t) + \xi(t)\,. \tag{42}$$

We assume the statistics of the random force are normal with a delta correlated correlation of strength D

$$\langle \xi(t)\xi(t')\rangle = 2D\delta(t-t')\,. \tag{43}$$

An alternative description of the dynamics is given by the evolution of the probability density in phase space where $P(z,t)dz$ is the probability that the dynamic variable $Z(t)$ has a value in the interval $(z, z+dz)$ at time t given a value $q(t)$ at the origin $z=0$. The phase space dynamics are formally expressed by the equation:

$$G\left(\frac{\partial}{\partial t}, \frac{\partial}{\partial z}\right) P(z,t) = q(t)\delta(z)\,. \tag{44}$$

The analytic function $G(\cdot,\cdot)$ of the indicated operators along with the inhomogeneous term $q(t)$ determine the dynamics of the process modeled by the *pdf*.

A phase space equation for a classical diffusion process with linear dissipation equivalent to Eq. (42) is determined by:

$$G\left(\frac{\partial}{\partial t}, \frac{\partial}{\partial z}\right) = \frac{\partial}{\partial t} - \frac{\partial}{\partial z}\left[\lambda z + D\frac{\partial}{\partial z}\right] \quad \text{and} \quad q(t) = 1\,. \tag{45}$$

The corresponding FPE is given by[217]:

$$\frac{\partial P(z,t|z_0,t_0)}{\partial t} = \frac{\partial}{\partial z}\left[\lambda z + D\frac{\partial}{\partial z}\right] P(z,t|z_0,t_0)\,, \tag{46}$$

where $P(z,t|z_0,t_0)dz$ is the probability that the dynamic variable lies in the phase space interval $(z+dz, z)$ at time t conditional on $Z(0)=z_0$ at time $t=t_0$. The solution to Eq. (46) for $t_0=0$ is given by:

$$P(z,t|z_0) = \frac{1}{\sqrt{4\pi\sigma^2(t)}} \exp\left[-\frac{(z-\langle z;t\rangle)^2}{2\sigma^2(t)}\right] \tag{47}$$

with average value $\langle z;t\rangle = z_0 e^{-\lambda t}$ and variance $\sigma^2(t) = D/\lambda(1-e^{-\lambda t})$. In the absence of dissipation the average value is constant and the variance grows linearly in time. However for finite dissipation the average decays exponentially in time and the variance approaches a constant value given by the ratio of the diffusion coefficient and the dissipation rate. If Z is the velocity of a Brownian particle the

variance would be proportional to the temperature of the surrounding fluid resulting in the Einstein relation $D/\lambda = k_B T$, see, for example, Fürth.[61]

Multiplicative fluctuations can be addressed by examining the FPE associated with a linear stochastic dissipation parameter.[118,193] Consider the nonlinear rate equation with multiplicative fluctuations

$$\frac{dX}{dt} = -\lambda X \ln X + \xi(t) X \tag{48}$$

for which the logarithmic transformation $Z = \ln X$ yields the rate equation with additive fluctuations $\xi(t)$ given by Eq. (42). The FPE for the transformed equation is Eq. (46) with the solution Eq. (47). In terms of the original variable the *pdf* is a log-normal distribution, for more details see Goel *et al.*[76]

5.1.2. *Stochastic ontogenetic growth model*

A more interesting rate equation was first considered by von Bertalanffy[219] who postulated a simple nonlinear rate equation to describe the growth of TBM m of the form

$$\frac{dm}{dt} = A_\eta m^\eta - C_\beta m^\beta \tag{49}$$

at time t where η and β are unspecified exponents, and A_η and C_β are positives constants. The solution to this equation was studied by von Bertalanffy[219] with $\eta = 2/3$ and $\beta = 1$. More recently West *et al.*[250] constructed Eq. (49), called an ontogenetic growth model (OGM), from a conservation of energy argument and obtained a universal curve from the solution and fit it to data by using $\eta = 3/4$ and $\beta = 1$. In the OGM the parameters are given by $C_\beta = B_m/E_m$ with B_m the metabolic rate required to maintain an existing unit of biomass; E_m the metabolic energy required to create a unit biomass and $A_\eta = a/E_m$. Banavar *et al.*[10] obtained an equivalent universal curve and fit the same data for both $\eta = 2/3, 3/4$ and $\beta = 1$. The OGM equation has the scaling form:

$$\frac{dm}{dt} = m^\eta f(m/M_0)\,, \tag{50}$$

where M_0 is chosen to be the maximum TBM that solves the stationary equation $dm/dt = 0$. The data from 13 organisms graphed as $r = (m/M_0)^{1-\eta}$ versus $\tau = -\ln(1-r)$ collapse onto a single universal curve[250] that is fit equally well with $\eta = 2/3$ or $\eta = 3/4$.[10]

West and West[246] generalized the OGM to incorporate the disordering influence of entropy by including the statistical fluctuations of the measured mass. The dynamics of such a stochastic process eventually erases the influence of the initial state and this gradual loss of information is a manifestation of increasing entropy. They refer to this as the stochastic ontogenetic growth model (SOGM). Consider a phenomenological Langevin equation with multiplicative fluctuations for the TBM where to avoid confusion we use the dummy variable $Z = m$, which is actually the

TBM for species i and individual j and individual j given by M_{ij}. Thus, we replace Eq. (49) for $\eta = b$ and $\beta = 1$ for the SOGM stochastic differential equation:

$$\frac{dZ}{dt} = A_b Z^b - C_0 Z + Z\xi(t)\,, \tag{51}$$

with $\xi(t)$ given by a delta correlated random process of strength D with normal statistics and correlations given by Eq. (43). Rather than assuming the rate of creating a unit biomass is a single number C_1 they assume it has a stochastic component: $C_1 \to C_0 + \xi(t)$, with average value C_0.

An equivalent description of the SOGM is given by the corresponding dynamics of the *pdf* in phase space. The FPE corresponding to Eq. (51) is[118,193]:

$$\frac{\partial P(z,t)}{\partial t} = \frac{\partial}{\partial z}\left[-(A_b z^b - C_0 z) + Dz\frac{\partial}{\partial z}z\right] P(z,t)\,. \tag{52}$$

The general solution to Eq. (52) remains a mystery, but the steady-state solution ($t \to \infty$) denoted by the ss subscript obtained by setting the probability flux to zero is given by:

$$P_{ss}(z) = \frac{\beta\gamma^{\frac{\mu-1}{\beta}}}{\Gamma\left(\dfrac{\mu-1}{\beta}\right)}\frac{\exp[-\gamma z^{-\beta}]}{z^{\mu}}\,; \tag{53}$$

normalized on the interval $(0,\infty)$ with the parameter values $\gamma = A_b/\beta D$, $\mu = 1 + (C_0/D)$ and $\beta = 1 - b$. Note that the steady-state solution to the SOGM FPE replaces the deterministic steady-state solution obtained from the OGM.[10,250]

West and West[246] fit the parameters in Eq. (53) to a data set of mammalian species tabulated by Heusner[91] and this fit is depicted in Fig. 11. They constructed a histogram by partitioning the mass axis into intervals of 20 g and counting the number of species within each interval. The vertical axis is the relative number of species as a function of TBM. The allometry exponet is fixed at $b = 3/4$ so that $\beta = 1/4$ and the remaining parameters are determined to have the best values of $\gamma = 13.4$ and $\mu = 2.04$ with a quality of fit measured by the correlation coefficient $r^2 = 0.96$.

Figure 11 shows the fit to the low-mass species out to 500 g. The remaining fit out to three million grams is not shown but is in fact the more ineresting part of the distribution. To capture this information on a single graph we[246] construct a second histogram, this one for the asymptotic region from approximately one thousand to three million grams. Figure 12 depicts the fit to the logarithmic histogram data points indicated by the dots starting at a TBM of 1.1 kg. An inverse power-law distribution would be a straight line with a negative slope on this log–log graph. Inserting the parameter values $\mu = 1.67$ and $\gamma - 8.96$ into the steady-state TBM *pdf* given by Eq. (53) yields the solid cuve in Fig. 12 which fits the data extremely well. The curve is quite clearly an inverse power law in the interspecies TBM. This coarse-grained description of the interspecies TBM statistics indicates great

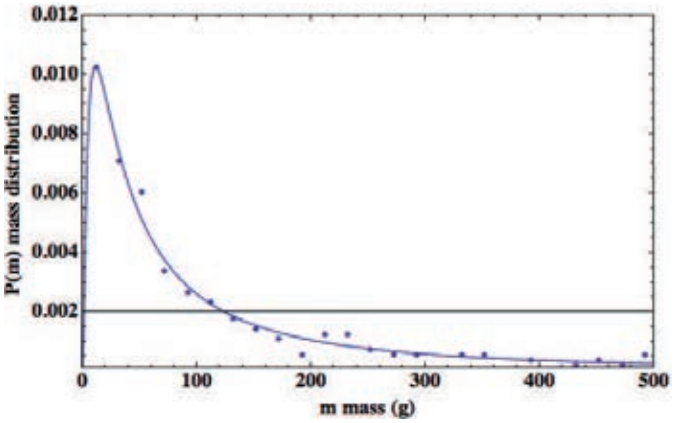

Fig. 11. The histogram constructed from the average TBM data for 391 mammalian species[91] is given by the dots. The mass data has been divided into intervals of 20 g each and the number of species within each such interval counted. The horizontal axis is the relative frequency in each interval and the solid line segment is the least squares fit of Eq. (53) to the data points. The quality of fit is $r^2 = 0.96$.[246]

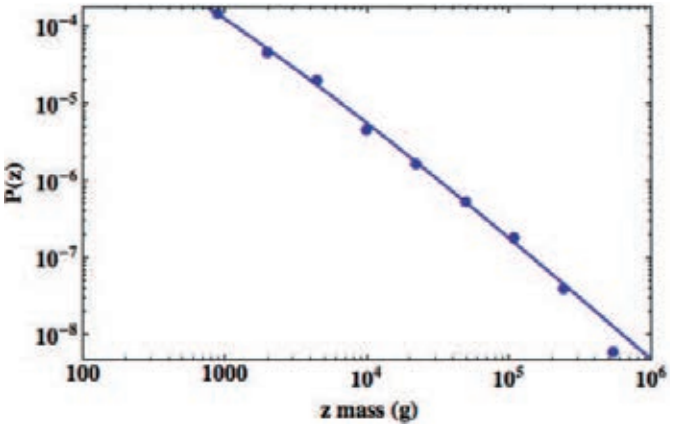

Fig. 12. The average TBM data for 391 mammalian species[91] are used to construct a histogram. The mass interval is divided into 20 equally spaced intervlas on a logarithm scale and the number of species within each interval counted. The least-square fit to the nine data points is then made using logrimically transformed distribution, see Ref. 246 for details. The quality of the fit is $r^2 = 0.998$.

variability particularly since $\mu < 2$ indicating that the variance of the interspecies TBM diverges.

5.1.3. *Interspecies AR derivation*

We[241,243] explicitly constructed a statistical theory of the fluctuations in the measured species metabolic rate B_i and TBM M_i to calculate the interspecies metabolic

AR. The strategy was to related the average BMR to the average TBM through the AR. This approach can be followed here from the long-time or steady-state average SOGM TBM using the steady-state *pdf*:

$$\langle z\rangle = \int_0^\infty z P_{ss}(z)dz = \frac{\beta\gamma^{\frac{\mu-1}{\beta}}}{\Gamma\left(\frac{\mu-1}{\beta}\right)}\int_0^\infty z^{1-\mu}\exp[-\gamma z^{-\beta}]dz$$

and replacing z with the TBM for species i reduces the average to:

$$\langle M_i\rangle = \gamma^{1/\beta}\frac{\Gamma\left(\frac{\mu-1}{\beta}-\frac{1}{\beta}\right)}{\Gamma\left(\frac{\mu-1}{\beta}\right)} \approx \left[\gamma\frac{\beta}{\mu-1}\right]^{1/\beta}. \tag{54}$$

Here we interpret the ensemble average in terms of an average over an ensemble of individual members of species i. In this equation we have approximated the ratio of gamma functions by an asymptotic value and substituting the parameter values into the right-hand side of Eq. (54) yields:

$$\langle M_i\rangle \approx \left(\frac{A_b}{C_0}\right)^{1/\beta} = \left(\frac{a}{B_m}\right)^{1/\beta}. \tag{55}$$

The equality in Eq. (55) is obtained by substituting the values of the parameters from OGM and using $b = 3/4$ and $\beta = 1/4$ to yield

$$B_m \approx a\langle M_i\rangle^{-1/4}. \tag{56}$$

Thus, the average metabolic rate necessary to maintain a unit biomass is dependent on the inverse quarter power of the average TBM of the species. This is the same expression obtained by Moses *et al.*[149] if we identify their adult TBM with the average TBM obtained from the steady-state *pdf* of the SOGM.

Note that the average TBM for species i replaces M_0 obtained from the $dm/dt = 0$ solution to Eq. (50). On the other hand the average BMR can be determined from the bth moment of the TBM

$$\begin{aligned}\langle B_i\rangle &= a\langle M_i^b\rangle = a\int_0^\infty z^b P_{ss}(z)dz \\ &= a\gamma^{-1+1/\beta}\frac{\Gamma\left(\frac{\mu-1}{\beta}+1-\frac{1}{\beta}\right)}{\Gamma\left(\frac{\mu-1}{\beta}\right)} \approx a\left[\gamma\frac{\beta}{\mu-1}\right]^{1/\beta-1}.\end{aligned} \tag{57}$$

Comparing this last equation with Eq. (54) allows us to write:

$$\langle B_i\rangle \approx a\langle M_i\rangle^{1-\beta} = a\langle M_i\rangle^b, \tag{58}$$

which is the interspecies metabolic AR. We emphasize[246] that the interspecies AR is a pheomenological equation that without the SOGM does not have a formal theoretical basis.

The SOGM constitutes the first theoretical construction of an interspecies metabolic AR starting from a fundamental dynamic equation and relating the proper averages. It is true that we used a nonlinear multiplicative Langevin equation, but the original dynamics stem from the conservation of energy argument[250] and the fluctuations are a consequence of the dynamics being degraded by entropy.[243] This suggests a possible untraveled path for future research in this area.

5.2. *Scaling solution for AR*

A phase space equation for anomalous diffusion containing the influence of long-term memory on the dynamics of the *pdf* was first discussed by West and Seshadri[227] in term of the fractional calulus. The resulting fractional diffusion equation[108,236] (FDE) has subsequently found a variety of uses in the physical sciences. The *pdf* that solves a class of FDEs satisfies the scaling equation

$$P(z,t) = \frac{1}{t^{\mu_z}} F_z\left(\frac{z}{t^{\mu_z}}\right) . \tag{59}$$

Note that this scaling of the *pdf* is also a realization of the RG relation for the random variable $Z(bt) = b^{\mu} Z(t)$.

The function $F_z(\cdot)$ in Eq. (59) is left unspecified but it is analytic in the similarity variable z/t^{μ}. As mentioned in the introduction a standard diffusion process $Z(t)$ is the displacement of the diffusing particle from its initial position at time t, and for vanishing small dissipation the scaling parameter is $\mu_z = 1/2$ and the functional form of $F_z(\cdot)$ is a normal distribution. However, for general complex phenomenon there is a broad class of distributions for which the functional form of $F_z(\cdot)$ is not Gaussian and the scaling index $\mu_z \neq 1/2$. For example, the α-stable Lévy process[147,184,198,264] scales in this way and the Lévy index is in the range $0 < \alpha \leq 2$, with the equality holding for the Gauss distribution and the scaling index is related to the Lévy index by $\mu_z = 1/\alpha$, see West, Geneston and Grigolini[239] and Uchaikin[216] for very different discussions of this scaling.

The Gibbs entropy (Shannon information),[23,197] can be defined using the *pdf* for the variable $Z(t)$ Eq. (59) to obtain:

$$S_z(t) = -\int P(z,t) \ln P(z,t) dz = S_z^0 + \mu_z \ln t \, , \tag{60}$$

so the entropy deviation from the reference state $S_z^0 \equiv -\int F_z(q) \ln F_z(q) dq$ integrated with respect to the scaled variable $q = z/t^{\mu_x}$, increases logarithmically in the independent variable t.

Huxley[98] assumed the differential growth equations in an organism to have the same form with proportional growth rates. West and West[241,243] adapted this assumption and presumed the two parts of an organism share the same class of probability densities that describe their interacting observables. Here t is clock time, the independent variable, and the network measures are the dependent variables,

the average of a generic scaling observable using the *pdf* given by Eq. (59) yields:

$$\langle Z(t)\rangle = \int zP(z,t)dz = t^{\mu_z}\int qF_z(q)dq = t^{\mu_z}\bar{Z}\,. \tag{61}$$

Note that $\bar{Z} = \int qF_z(q)dq$ is a finite, time-independent constant. Comparing Eqs. (61) and (60) enables us to write for the change in entropy relative to a reference state:

$$\Delta S_z = \ln[\langle Z(t)\rangle/\bar{Z}] \tag{62}$$

so that the change in the average value of an observable is determined by the change in entropy

$$\langle Z(t)\rangle = \bar{Z}e^{\Delta S_z(t)}\,. \tag{63}$$

Consequently Z may be identified with either of the network variables to obtain the relation between entropies from Eq. (60)

$$\Delta S_x/\mu_x = \Delta S_y/\mu_y$$

and using Eq. (63) we can write:

$$\langle Y_i\rangle = \bar{Y}e^{\Delta S_y} = \bar{Y}e^{\frac{\mu_y}{\mu_x}\Delta S_x} = a\langle X_i\rangle^b \tag{64}$$

with the allometry coefficient given by $a = \bar{Y}/\bar{X}^b$ and the allometry exponent by $b = \mu_y/\mu_x$. We have again introduced the index for the single species i to emphsize that this is the interspecies AR. This derivation of the empirical interspecies AR is solely a consequence of the scaling properties of the *pdf*'s.

The rate of entropy generation is determined by the time derivative of Eq. (63) for X and Y and substituting from the entropy balance equation yields:

$$\frac{1}{\mu_x\langle X_i\rangle}\frac{d\langle X_i\rangle}{dt} = \frac{1}{\mu_y\langle Y_i\rangle}\frac{d\langle Y_i\rangle}{dt}\,. \tag{65}$$

Equation (65) shows the correspondence of the probabilistic approach to AR with that of Huxley, with the dynamic variables of individual species members replaced by averages over an ensemble of individuals. In the present case the allometry exponent is now the ratio of the power-law indices in the *pdf*'s, which from Eq. (65) can also be interpreted as the ratio of growth rates. Moreover, the allometry coefficient is determined by the scaling functions in the *pdf*'s. It is the average response or adaptation of the subnetwork to the average behavior of the host network that is captured by the interspecies AR through the balance of the entropy generated. Moreover it is the scaling in the *pdf* and not necessarily geometric scaling of fractal networks that is the origin of the physiologic AR. Underlying this derivation is the assumption made earlier that this is an information-dominated network and is consequently driven by information (entropy) gradients and not the energy gradient necessary in the fractal geometry derivation of nutrient transport.

6. Conclusion

The statistical analysis of the metabolic data presented herein show that empirical ARs exist across multiple species and consequently the form of ARs are not solely dependent on species specific mechanisms. Moreover we have shown there is no universal value for the allometry exponent for three reasons. First there is the variability in the values of the allometry exponent obtained from data analysis in Sec. 3. We could rehash the arguments here, but an objective observer would have to conclude that although there are indications that a particular value might be strongly indicated in a specific context, the evidence for universality is not compelling. Even in the case of metabolic ARs one could reasonably make a case of $b = 2/3$ for small animals, $b = 3/4$ for large animal and $b = 1$ for plants, but no one value of b that spans the total range of animal and plant sizes. Second, the only theories that predict a universal value of the allometry exponent do so to explain the intraspecies AR and not the interspecies AR. There is no first principles theory that derives the empirical AR between the averaged observables. The phenomenological theory presented in Section 4 successfully derives the interspecies AR and treats the allometry coefficient and allometry exponent as empirical parameters determined by the parameters in the *pdf*'s. Third and last the allometry exponent and coefficient are determined to co-vary using theory[243] and statistical data analysis.[72]

However let us not be too critical of phenomenological theories. Recall that thermodynamics is a phenomenological theory that has enjoyed remarkable success in explaining a plethora of complex physical phenomena. Even so the physics community has not yet been able to derive thermodynamics from the more reductionist (fundamental) statistical mechanics, so that a mechanistic understanding of thermodynamics remains controversial. By the same token the phenomenological theory of AR presented herein takes the discussion of AR out of the domain of the reductionist approaches previously used to derive the intraspecies ARs and refocuses it on the statistical properties of the empirical interspecies ARs. These analyses indicate a new avenue for the study of physiologic ARs, one that systematically includes both deterministic and statistical aspects using the probability calculus. This new perspective indicates that the origins of physiologic AR reside in the scaling properties of the *pdf*'s for nested complex networks.

In simple physical phenomena the dynamics of a network coupled to the environment is described by a Langevin equation, which is a stochastic differential equation. This mechanical description of the dynamics is equivalent to the phase space dynamics of the *pdf* such as given by the FPE. As the network becomes more complex its past history becomes more and more influential until finally the FPE must be replaced with a FDE and the dynamics are the domain of the fractional calculus. As we saw in Sec. 5 the general solution to a class of FDE's is a scaling *pdf* implying that ARs can result from scaling in the statistical dynamics of the phenomenon. The influence of the history of the growth of an organism on the growth

of an organ leads to intraspecies AR; the history of the size of an organism on the metabolic rate of the organism across species leads to interspecies AR.

The arguments in Sec. 5 imply that empirical ARs are a consequence of information transfer between complex information-dominated networks. Of course we have not rigorously proven that the entropy decrease (information increase) in the host network and the increase in entropy (information decrease) in the subnetwork have the relations assumed, this remains to be done. However the empirical relations are consistent with the Principle of Complexity Management in which the transfer of information between two complex information-dominated networks has been shown[7,239] to proceed from the network with the greater information content to the network with the lesser.

The phenomenological theory of empirical AR presented herein incorporates both stochastic and reductionistic mechanisms. From this approach we conclude that the empirical AR for the BMR, the life time of an organism and the myriad of other complex phenomena are not completely explained by reductionistic mechanisms. In particular the allometry parameters are determined not to be universal. This was supported by the demonstration that the allometry exponent and coefficient co-vary. On the other hand, the laws from the theory of probability can have universal forms without having universal parameters, for example the Law of Frequency of Errors and the Law of Large Numbers. The empirical AR is in part a consequence of the generic statistical behavior of complex networks that depend on the infinitely divisible nature of the *pdf*.[74,75] The phenomenological theory of AR presented herein is the application of the probability calculus to the understanding of the origins of the empirical relations between averages of different parts of a complex network. Consequently empirical AR is a manifestation of a law whose origin can be traced back to the probability calculus and the balancing of deterministic and stochastic mechanisms.

References

1. R. Adrian, *Analyst Math. Museum* **1**, 93 (1809).
2. P. Alberch *et al.*, *Paleobiology* **5**, 296 (1979).
3. R. Albert and A.-L. Barabasi, *Rev. Mod. Phys.* **74**, 48 (2002).
4. P. Allegrini *et al.*, *Front. Physiol.* **1**, 28 (2010) doi:10.3389/fphys.2010.00128.
5. P. S. Agutter and J. A. Tuszynski, *J. Exp. Biol.* **214**, 1055 (2011).
6. M. E. F. Apol, R. S. Etienne and H. Olff, *Funct. Ecol.* **22**, 1070 (2008).
7. G. Aquino *et al.*, *Phys. Rev. Lett.* **105**, 069901 (2010).
8. P. Bak and S. Boettcher, *Physica D* **107**, 143 (1997).
9. F. J. Ballard, R. W. Hanson and D. S. Kronfeld, *Fed. Proc.* **28**, 218 (1969).
10. J. R. Banavar *et al.*, *Nature* **420**, 626 (2002).
11. J. R. Banavar *et al.*, *Nature* **421**, 713 (2003).
12. J. R. Banavar *et al.*, *Phys. Rev. Lett.* **98**, 068104 (2007).
13. G. I. Barenblatt, *Scaling Phenomena in Fluid Mechanics* (Cambridge University Press, Cambridge, 1994).
14. G. I. Barenblatt and A. S. Monin, *Proc. Nat. Acad. Sci. USA* **99**, 10506 (1983).
15. M. Barnsley, *Fractals Everywhere* (Academic Press, Boston, 1988).

16. D. S. Bassett *et al.*, *PLoS Comp. Biol.* **6**, 1 (2010).
17. J. B. Bassingthwaighte, L. S. Liebovitch and B. J. West, *Fractal Physiology* (Oxford University Press, New York, 1994).
18. V. Beiu and W. Ibrahim, *Proc. IEEE ISCAS* 640 (2008).
19. A. Belgrano *et al.*, *Ecol. Lett.* **5**, 611 (2002).
20. J. Beran, *Statistics of Long-Memory Processes, Monographs on Statistics and Applied Probability*, Vol. 61 (Chapman & Hall, New York, 1994).
21. F. Bokma, *Funct. Ecol.* **18**, 184 (2004).
22. H. Boxenbaum, *J. Pharmacokin. Biopharm.* **10**, 201 (1982).
23. L. Brillouin, *Science and Information Theory* (Academic Press, New York, 1962).
24. S. Brody, *Bioenergetics and Growth* (Reinhold, New York, 1945).
25. J. H. Brown, *Macroecology* (University of Chicago Press, Chicago, IL, 1995).
26. J. H. Brown *et al.*, *Phil. Trans. R. Soc. Lond. B* **357**, 619 (2002).
27. J. H. Brown *et al.*, *Ecology* **85**, 1771 (2004).
28. J. H. Brown, G. B. West and B. J. Enquist, *Funct. Ecol.* **19**, 735 (2005).
29. J. Brownlee, *J. Roy. Soc. Stat. Soc.* **83**, 280 (1920).
30. M. Buchanan, *Nexus* (W. W. Norton, New York, 2002).
31. W. W. Calder III, *Size, Function and Life History* (Harvard University Press, Cambridge, MA, 1984).
32. C. G. Caro *et al.*, *The Mechanics of Circulation* (Oxford University Press, Oxford, 1978).
33. M. A. Changizi, *Biol. Cybern.* **84**, 207 (2001).
34. G. Cuvier, *Recherches sur les ossemens fossils* (Paris, 1812).
35. J. E. Cohen, T. Jonsson and S. R. Carpenter, *Proc. Nat. Acad. Sci. USA* **100**, 1781 (2003).
36. E. D. Cope, *The Primary Factors of Organic Evolution* (Open Court Publishing Company, 1896).
37. H. Cyr, Indvidual energy use and he allometry of population density, in *Scaling in Biology*, eds. J. H. Brown and G. B. West (Oxford University Press, New York, 2000), pp. 267–295.
38. H. Cyr and S. C. Walker, *Ecology* **85**, 1802 (2004).
39. J. Damuth, *Nature* **290**, 699 (1981a).
40. J. Damuth, *Biol. J. Linn. Soc.* **15**, 185 (1981b).
41. C. A. Darveau *et al.*, *Nature* **417**, 166 (2002).
42. C. A. Darveau *et al.*, *Nature* **421**, 714 (2003).
43. T. H. Dawson, *Science* **281**, 751a (1998).
44. L. Demetrius, S. Legendre and P. Harrenöes, *Bull. Math. Biol.* **71**, 800 (2009).
45. T. G. Dewey, *Fractals in Molecular Biophysics* (Oxford University Press, Oxford, 1997).
46. P. S. Dodds and D. H. Rothman, *Ann. Rev. Earth Planet Sci.* **28**, 1 (2000).
47. P. S. Dodds, D. H. Rothman and J. S. Weitz, *J. Theor. Biol.* **209**, 9 (2001).
48. E. Dubois, *Bull. Soc. Anthropol.* (*Paris*) **8**, 337 (1897).
49. C. M. Duarte, S. Agustin and R. H. Peters, *Oecologia* **74**, 272 (1987).
50. A. Einstein, *Ann. Phys.* **22**, 180 (1907).
51. N. Eldredge, *Time Frames* (Princeton University Press, Princeton, NH 1985).
52. N. Eldredge and S. J. Gould, Punctuated equilibria: an alternative to phyletic gradualism, in *Models in Paleobiology*, ed. T. J. M. Schopf (Freeman, Cooper and Co., San Francisco, CA, 1972), pp. 82–115.
53. B. J. Enquist, *Tree Phys.* **22**, 1045 (2002).
54. R. S. Etienne, M. E. Apol and H. Olff, *Funct. Ecol.* **20**, 394 (2006).

55. K. Falconer, *Fractal Geometry* (John Wiley, New York, 1990).
56. W. Farr, *J. Stat.* (*Lond*) **9**, 17 (1841).
57. J. Feder, *Fractals* (Plenum, New York, 1988).
58. H. A. Feldman and T. A. McMahon, *Resp. Physiol.* **52**, 149 (1983).
59. W. T. Fitch, *Zoology* **103**, 40 (2000).
60. Y. C. Fung, *Biodynamics* (Springer-Verlag, New York, 1984).
61. R. Fürth, *Investigations on the Theory of the Brownian Movement* by Albert Einstien, Ph.D., (1926), translated by A. D. Cowper (Dover, New York, 1956).
62. G. Galileo, This is in the Dialogue of the Second Day in *the Discorsi of 1638*, the work Galileo wrote while under house arrest by the Inquisition. It was translated as *Dialogues Concerning Two New Sciences* by H. Crew and A De Salvor in 1914 and reprinted by Dover, New York (1952).
63. F. Galton, *Proc. R. Soc. London* **29**, 365 (1879).
64. F. Gauss, *Theoria motus corporum coelestrium*, (Hamburg, Dover, 1809); Eng. Trans., *Theory of Motion of Heavenly Bodies Moving about the Sun in Conic Sections*, New York, 1963).
65. J. Gayon, *Am. Zool.* **40**, 748 (2000).
66. P. D. Gingerich, *J. Theor. Biol.* **204**, 201 (2000).
67. L. R. Ginzburg, O. Burger and J. Damuth, *Biol. Lett.* **6**, 850 (2010).
68. T. Gisiger, *Biol. Rev.* **76**, 161 (2001).
69. P. Glansdorf and I. Prigogine, *Thermodyanmic Theory of Structure, Stability and Function* (Wiley, New York, 1971).
70. N. R. Glass, *J. Fish Res. Board Can.* **26**, 2643 (1969).
71. D. S. Glazier, *Biol. Rev.* **80**, 611 (2005).
72. D. S. Glazier, *BioScience* **56**, 325 (2006).
73. D. S. Glazier, *Biol. Rev.* **85**, 111 (2010).
74. B. V. Gnedenko and A. N. Kolmogorov, *Limit Distributions for Sums of Independent Random Variables*, translated from Russian by K. L. Chung (Addison-Wesley, Reading, MA, 1954).
75. B. V. Gnedenko, *The Theory of Probability*, translated by B. D. Seckler (Chelsea Pub., New York, 1962).
76. N. S. Goel, S. C. Maitra and E. W. Montroll, *Rev. Mod. Phys.* **43**, 231 (1971).
77. A. L. Goldberger *et al.*, *Biophys. J.* **48**, 525 (1985).
78. A. Goldbeter, *Biochemical Oscillations and Cellular Rhythms* (Cambridge University Press, New York, 1996).
79. S. J. Gould, *Biol. Rev. Cam. Philos. Soc.* **41**, 587 (1966).
80. S. J. Gould, *Am. Natur.* **105**, 113 (1971).
81. J. H. Graham *et al.*, *Biol. J. Linn. Soc.* **80**, 57 (2003).
82. R. A. Groat, *Federation Proc.* **7**, 45 (1948).
83. J. T. Hack, *US Geol. Surv. Prof. Pap.* **294-B**, 52 (1957).
84. J. M. Hausdorff *et al.*, *J. Appl. Physiol.* **80**, 1448 (1996).
85. L. C. Hayek and M. A. Buzas, *Surveying Natural Populations* (Columbia University Press, New York, 1997).
86. A. M. Hemmingsen, *Rep. Steno. Mem. Hosp.* (*Copenhagen*) **4**, 1 (1950).
87. A. M. Hemmingsen, *Rep. Steno. Memor. Hosp. Nork. Insul.* **9**, 1 (1960).
88. S. C. Hempleman *et al.*, *J. Exp. Biol.* **208**, 3065 (2005).
89. W. R. Hess, *Archiv Anat. Physiol.* 1 (1914).
90. A. A. Heusner, *Resp. Physiol.* **48**, 1 (1982).
91. A. A. Heusner, *J. Exp. Biol.* **160**, 25 (1991).
92. A. V. Hill, *Proc. Roy. Soc. London Ser. B* **126**, 136 (1938).

93. A. V. Hill, *Sci. Prog.* **38**, 209 (1950).
94. M. A. Hofman, *Brain Behav. Evol.* **27**, 28 (1985).
95. R. E. Horton, *Geol. Soc. Amer. Bull.* **56**, 275 (1945).
96. N. A. Humphreys (ed.), *Vital Statistics: A Memorial Volume of Selections from the Reports and Writings of William Farr* (The Sanitory Institute of Great Britian, London, 1885).
97. T.-M. Hu and W. L. Hayton, *AAAPS Pham. Sci.* **3**, 1 (2001).
98. J. S. Huxley, *Problems of Relative Growth* (Dial Press, New York, 1931).
99. H. J. Jerison, *Science* **133**, 1012 (1961).
100. H. J. Jerison, Allometry, brain size, cortical surface, and convolutedness, in *Primate Brain Evolution*, (eds.) E. Armstrong and O. Falk (Plenum, New York, 1982), pp. 77–84.
101. J. H. Jones, *Comp. Biochem. Physiol. B* **120**, 125 (1998).
102. T. Jonsson, J. E. Cohen and S. R. Carpenter, *Adv. Ecol. Res.* **36**, 1 (2005).
103. L. P. Kadanoff *et al.*, *Rev. Mod. Phys.* **39**, 395 (1967).
104. P. Kaitaniemi, *PLoS ONE* **3**(4), e1932 (2008).
105. A. Kamiya, T. Togawa and A. Yamamoto, *Bull. Math. Biol.* **36**, 311 (1974).
106. A. J. Kerkhoff and B. J. Enquist, *J. Theor. Biol.* **257**, 519 (2009).
107. H. Kitaoka and B. Suki, *J. Appl. Physiol.* **82**, 968 (1997).
108. J. Klafter and R. Metzler, *Phys. Rept.* **339**, 1 (2000).
109. M. Kleiber, *Hilgarida* **6**, 315 (1932).
110. T. Kolokotrones *et al.*, *Nature* **464**, 753 (2010).
111. P. Kopletz, L. Bartosch and L. Schütz, in *Introduction to Functional Renormalization Group*, Lectures in Physics, Vol. 798 (Springer, Berlin, 2010).
112. J. Kozlowski and J. Weiner, *Am. Natur.* **149**, 352 (1997).
113. J. Kozlowski and M. Konarzewski, *Funct. Ecol.* **18**, 283 (2004).
114. J. Kozlowski and M. Konarzewski, *Funct. Ecol.* **19**, 739 (2005).
115. F. A. Labra, P. A. Marquet and F. Bozinovic, *PNAS* **104**, 10900 (2007).
116. P. S. Laplace, *Analytic Theory of Probabilities* (Paris, 1810).
117. P. Langevin, *Comtes Rendus Acad. Sci.* **146**, 530 (1908).
118. K. Lindenberg and B. J. West, *The Nonequilibrium Statistical Mechanics of Open and Closed Systems* (pnVCH, New York, 1990).
119. S. L. Lindstedt and W. A. Calder III, *The Condor* **78**, 91 (1976).
120. S. L. Lindstedt and W. A. Calder III, *Quart. Rev. Biol.* **36**, 1 (1981).
121. S. L. Lindstedt, B. J. Miller and S. W. Buskirk, *Ecology* **67**, 413 (1986).
122. S. L. Lindstedt and P. J. Schaeffer, *Lab. Anim.* **36**, 1 (2002).
123. E. N. Lorenz, *J. Atmos. Sci.* **20**, 130 (1963).
124. E. N. Lorenz, *The Essence of Chaos* (University of Washington Press, Seattle, 1993).
125. C. Lyell, *Principles of Geology* (James Kay Jun & Brother, Philadelphia, 1837).
126. R. L. Magin, *Fractional Calculus in Bioengineering* (Begell House, CN, 2006).
127. I. Mahmood, *Life Sci.* **63**, 2365 (1998).
128. A. M. Makarieva, *J. Theor. Biol.* **237**, 291 (2005a).
129. A. M. Makarieva, V. G. Gorshkov and B.-L. Li, *Ecol. Comp.* **2**, 259 (2005b).
130. R. D. Manaster and S. Manaster, *J. Morphol.* **147**, 299 (1975).
131. B. B. Mandelbrot, *Fractals, Form and Chance* (W.H. Freeman San Francisco, CA, 1977).
132. B. B. Mandelbrot, *The Fractal Geometry of Nature* (W.H. Freeman, San Francisco, CA, 1982).
133. B. B. Mandelbrot, Self-affine fractal sets, in *Fractals in Physics*, eds. L. Pietronero and E. Tosatti (North-Holland, Amsterdam, 1986), pp. 3–28.

134. B. B. Mandelbrot, *Fractals and Scaling in Finance* (Springer, New York, 1997).
135. R. N. Mantegna and H. E. Stanley, *Econophysics* (Cambridge University Press, New York, 2000).
136. A. Maritan *et al.*, *Geophys. Res. Lett.* **29**, 1508 (2001).
137. R. D. Martin and P. H. Harvey, Brain size allometry: Ontogeny and phylogeny, in *Size & Scaling in Primate Biology*, ed. W. L. Jungers (Plenum Press, New York, 1985).
138. B. Mauroy *et al.*, *Nature* **427**, 633 (2004).
139. T. A. McMahon, *Science* **179**, 1201 (1973).
140. T. A. McMahon, *Amer. Nat.* **109**, 547 (1975).
141. B. K. McNab, *The Physiological Ecology of Vertebrates: A View from Energetics* (Comstock Publ. Ass., 2002).
142. B. K. McNab, *Comp. Biochem. Physiol.* **152**, 22 (2009).
143. P. Meakin, *Fractals, Scaling and Growth Far from Equilibrium* (Cambridge University Press, Cambridge, 1998).
144. K. S. Miller and B. Ross, *An Introduction to the Fractional Calculus and Fractional Differential Equations* (John Wiley & Sons, New York, 1993).
145. C. O. Mohr, *Am. Midl. Nat.* **24**, 581 (1940).
146. D. R. Montgomery and W. E. Dierich, *Science* **255**, 826 (1992).
147. E. W. Montroll and B. J. West, On an enriched collection of stochastic processes, in *Fluctuation Phenomena*, eds. E. W. Montroll and J. L. Lebowitz, Studies in Statistical Mechanics, Vol. VII (North-Holland, Amsterdam, 1979).
148. E. W. Montroll and M. F. Shlesinger, *J. Stat. Phys.* **32**, 209 (1983).
149. M. E. Moses *et al.*, *J. R. Soc. Interface* **5**, 1469 (2008).
150. C. D. Murray, *Proc. Nat. Acad. Sci. USA* **12**, 207 (1926a).
151. C. D. Murray, *J. Gen. Physiol.* **9**, 835 (1926b).
152. T. R. Nelson, B. J. West and A. L. Goldberger, *Experientia* **46**, 251 (1990).
153. M. E. J. Newman, *SIAM Rev.* **45**, 167 (2003).
154. K. J. Niklas, *Biol. Rev.* **79**, 871 (2004).
155. E. Ott, *Chaos in Dynamical Systems* (Cambridge University Press, New York, 1993).
156. G. C. Packard, *J. Theor. Biol.* **257**, 515 (2008).
157. G. C. Packard and T. J. Boardman, *Physiol. Biochem. Zool.* **81**, 496 (2008).
158. P. R. Painter, *Theor. Biol. Med. Model.* **2**, 31 (2005).
159. S. Peckham, *Water Resources Res.* **31**, 1023 (1995).
160. S. D. Peckham and V. K. Gupta, *Water Resources Res.* **35**, 2763 (1999).
161. C.-K. Peng *et al.*, *Phys. Rev. Lett.* **70**, 1343 (1993).
162. R. H. Peters, *The Ecological Implications of Body Size* (Cambridge University Press, Cambridge, 1983).
163. C. G. Phillips, S. R. Kaye and R. C. Schroter, *Respir. Physiol.* **98**, 193-217 (1994).
164. D. Pilbeam and S. J. Gould, *Science* **186**, 892 (1974).
165. R. E. Plotnick and J. J. Sepkoski, *Paleobiol.* **27**, 126 (2001).
166. F. W. Preston, *Ecology* **43**, 185 (1962).
167. J. W. Prothero, *J. Brain Res.* **38**, 513 (1997).
168. C. A. Price, B. J. Enquist and V. M. Savage, *PNAS* **104**, 13204 (2007).
169. I. Prigogine and I. Stengers, *Order Out of Chaos: Man's New Dialogue With Nature* (Bantam Books, Toronto, 1984).
170. C. L. Que *et al.*, *J. Appl. Physiol.* **91**, 1131 (2001).
171. O. G. Raabe *et al.*, *Tracheobronchial Geometry: Human, Dog, Rat, Hamster* (Lovelace Foundation for Medical Education and Research, Albuquerque, 1976).

172. N. Rashevsky, *Mathatical Biophysics Physico-Mathematical Foundations of Biology*, Vol. 2, 3rd edn. (Dover Publications, New York, 1960).
173. D. M. Raup and J. J. Skepkoski Jr., *Science* **215**, 1501 (1982).
174. P. B. Reich *et al.*, *Nature* **439**, 457 (2006).
175. L. E. Reichl, *A Modern Course in Statistical Physics* (John Wiley & Sons, New York, 1998).
176. M. J. Reiss, *The Allometry of Growth and Reproduction* (Cambridge University Press, Cambridge, 1989).
177. J. P. Richter (ed.) *The Notebooks of Leonardo da Vinci*, Vol. 1 (Dover, New York, 1970); unabridged edition of the work first published in London in 1883.
178. R. Rigon, I. Rodriguez-Iturbe and A. Rinaldo, *Water Resources Res.* **32**, 3367 (1998).
179. P. A. Rikvold and R. K. P. Zia, *Phys. Rev. E* **68**, 031913 (2003).
180. H. U. Riisgård, *Ecol. Lett.* **1**, 71 (1998).
181. A. Rinaldo, J. R. Banavar and A. Maritan, *Water Resources Res.* **42**, 1 (2006).
182. I. Rodriguez-Iturbe and A. Rinaldo, *Fractal River Basins, Chance and Self-organization* (Cambridge University Press, Cambridge, UK, 1997).
183. M. Rubner, *Z. Biol.* **19**, 353 (1883).
184. G. Samorodnitsky and M. S. Taqqu, *Stable Non-Gaussian Random Processes* (Chapman & Hall, New York, 1994).
185. G. A. Sacher, Relation of lifespan to brain weight and body weight in mammals, in *Ciba Foundation Colloquium on Aging*, Vol. 1, ed. G. E. W. Wolstenholme (1959).
186. B. S. Sagar and T. L. Tien, *Geophys. Res. Lett.* **31**(1-4), L06501 (2004).
187. B. Sapoval, *Universalitiés et Fractales* (Flammarion, Paris, 1997).
188. S. et Rameaux, *Bull. Acad. R. Med.* (*Paris*) **3**, 1094 (1838–39).
189. V. M. Savage *et al.*, *Funct. Ecol.* **18**, 257 (2004).
190. V. M. Savage, E. J. Deeds and W. Fontana, *PLoS Compt. Biol.* **4**(9), e1000171 (2008).
191. Y. Sawada *et al.*, *J. Pharmacokin Biopharm.* **12**, 241 (1984).
192. A. E. Scheidegger, *Bull. Int. Assoc. Sci. Hyd.* **XV**, 1 (1970).
193. A. Schenzle and H. Brand, *Phys. Rev. E* **20**, 1628 (1979).
194. G. Schlenska, *J. Hirnforsch* **15**, 401 (1974).
195. K. Schmidt-Nielsen, *Scaling, Why is Animal Size so Important?* (Cambridge University Press, Cambridge, 1984).
196. K. Schmidt-Nielsen, *Animal Physiology* (Cambridge University Press, Cambridge, 1997).
197. E. Schrödinger, *What is Life?*, Based on lectures delivered under the auspices of the Dublin Institute for Advanced Studies at Trinity College, Dublin, in February 1943.
198. V. Seshadri and B. J. West, *Proc. Nat. Acad. Sci. USA* **79**, 4501 (1982).
199. B. Shea, *Am. J. Phys. Anthopol.* **56**, 179 (1981).
200. M. F. Shlesinger and B. J. West, *Phys. Rev. Lett.* **67**, 2106 (1991).
201. J. K. L. da Silva, G. J. M. Garcia and L. A. Barbosa, *Phys. Life Rev.* **3**, 229 (2006).
202. R. J. Smith, *J. Theor. Biol.* **87**, 97 (1980).
203. R. J. Smith, *Am. J. Phys. Anthropol.* **90**, 215-228 (1993).
204. O. Snell, *Arch. Psychiatr.* **23**, 436 (1892).
205. K. Snell (ed.), *Understanding the Control of Metabolism* (Portland, London, 1997).
206. K. Sneppe *et al.*, *Proc. Nat. Acad. Sci. USA* **92**, 5209 (1995).
207. I. M. Sokolov, J. Klafter and A. Blumen, *Phys. Today Nov.* 48 (2002).
208. R. V. Solé *et al.*, *Nature* **388**, 764 (1997).
209. C. F. Stevens, *J. Biol.* **8**, 14 (2009).
210. L. R. Taylor, *Nature* **189**, 732 (1961).

211. C. R. Taylor and I. P. Woiwod, *J. Animal Ecol.* **49**, 209 (1980).
212. C. R. Taylor and E. R. Weibel, *Respir. Physiol.* **44**, 1 (1981).
213. D. W. Thompson, *On Growth and Form*, 2nd. edn. (Cambridge University Press, Cambridge, 1963).
214. D. B. Tower, *J. Comp. Neurol.* **101**, 9 (1954).
215. D. L. Turcotte, *Fractals and Chaos in Geology and Geophysics* (Cambridge University Press, Cambridge, 1992).
216. V. V. Uchaikin, *Int. J. Theor. Phys.* **39**, 3805 (2000).
217. G. W. Uhlenbeck and L. S. Ornstein, *Phys. Rev.* **36**, 823 (1930).
218. M. O. Vlad *et al.*, *PNAS* **104**, 4798 (2007).
219. L. Von Bertalanffy, *Q. Rev. Biol.* **32**, 217 (1957).
220. D. I. Warton, *Biol. Rev.* **85**, 259 (2006).
221. D. J. Watts, *Small Worlds* (Princeton University Press, Princeton, NJ, 1999).
222. E. R. Weibel and D. M. Gomez, *Science* **137**, 577 (1962).
223. E. R. Weibel, *Symmorphosis: On Form and Function in Shaping Life* (Harvard University Press, Cambridge, 2000).
224. E. R. Weibel, *Nature* **417**, 131 (2002).
225. M. B. Weissman, *Rev. Mod. Phys.* **60**, 537 (1988).
226. G. Werner, *Front. Physiol.* **1**, 15 (2010) doi:10.3389/fphys.2010.00015.
227. B. J. West and V. Seshadri, *Physica A* **113**, 293 (1982).
228. B. J. West, V. Barghava and A. L. Goldberger, *J. Appl. Physiol.* **60**, 1089 (1986).
229. B. J. West and A. L. Goldberger, *Am. Sci.* **75**, 354 (1987).
230. B. J. West, in *Fractal Physiology and Chaos in Medicine*, Studies of Nonlinear Phenomena in Life Science Vol. 1 (World Scientific, Singapore, 1990a).
231. B. J. West, *Ann. Biomed. Eng.* **18**, 135 (1990b).
232. B. J. West, *Int. J. Mod. Phys. B* **4**, 1629 (1990c).
233. B. J. West and M. Shlesinger, *Am. Sci.* **78**, 40 (1990d).
234. B. J. West, in *The Lure of Modern Science: Fractal Thinking*, Studies of Nonlinear Phenomena in Life Science, Vol. 3 (World Scientific, Singapore, 1999a).
235. B. J. West, *Physiology, Promisucity and Prophecy at the Millennium: A Tale of Tails*, Studies of Nonlinear Phenomena in Life Science, Vol. 7 (World Scientific, Singapore, 1999b).
236. B. J. West, M. Bologna and P. Grigolini, *Physics of Fractal Operators* (Springer, Berlin, 2003).
237. B. J. West and L. A. Griffin, *Biodynamics: Why the Wirewalker Doesn't Fall* (John Wiley & Sons, Hoboken, 2004).
238. B. J. West, in *Where Medicine Went Wrong*, Studies of Nonlinear Phenomena in Life Science, Vol. 11 (World Scientific, Singapore, 2006).
239. B. J. West, *Phys. Rept.* **468**, 1 (2008).
240. B. J. West, *Front. Physiol.* **1**, 12 (2010) doi:10.3389/fphys.2010.00012.
241. B. J. West and D. West, Origin of allometry hypothesis, in *Fractional Dynamics*, eds. J. Klafter, S. C. Lin and R. Metzler (World Scientific, Singapore, 2012).
242. D. West and B. J. West, *Physica A* **390**, 1733 (2011).
243. D. West and B. J. West, *Europhys. Lett.* **94**, 38005 (2011).
244. B. J. West and P. Grigolini, *Complex Webs: Anticipating the Improbable* (Cambridge University Press, Cambridge, 2011).
245. B. J. West and D. West, *Fractional Calculus Appl. Anal.* **15**, 127 (2012).
246. B. J. West and D. West, *Europhys. Lett.* **97**, 48002 (2012).
247. G. B. West, J. H. Brown and B. J. Enquist, *Science* **276**, 122 (1997).
248. G. B. West, *Physica A* **263**, 104 (1999).

249. G. B. West *et al.*, The origin of universal scaling laws in biology, in *Scaling in Biology*, eds. J. H. Brown and G. B. West (Oxford University Press, Oxford, 2000), pp. 87–112.
250. G. B. West, J. H. Brown and B. J. Enquist, *Nature* **413**, 628 (2001).
251. G. B. West *et al.*, *Nature* **421**, 712 (2003).
252. G. B. West and J. H. Brown, *Phys. Today*, 36 (2004).
253. J. F. White and S. J. Gould, *Am. Natur.* **99**, 5 (1965).
254. C. R. White and R. S. Seymour, *J. Exp. Biol.* **208**, 1611 (2005).
255. C. R. White, P. Cassey and T. M. Blackburn, *Ecology* **88**, 315 (2007).
256. C. B. Williams, *Patterns in the Balance of Nature and Related Problems in Quantitative Ecology* (Academic Press, New York, 1964).
257. R. J. Williams and N. D. Martinez, *Eur. Phys. J. B* **38**, 297 (2004).
258. J. C. Willis, *Age and Area* (Cambridge University Press, Cambridge, 1922).
259. K. G. Wilson, *Rev. Mod. Phys.* **47**, 773 (1975).
260. T. A. Wilson, *Nature* 668 (1967).
261. G. Woodward *et al.*, *TRENDS Ecol. Evol.* **20**, 402 (2005).
262. P. Yodzis and S. Innes, *Am. Nat.* **139**, 1151 (1992).
263. J. H. Zar, *BioScience* **18**, 1118 (1968).
264. V. M. Zolotarev, *One-dimensional Stable Distributions, Translation of Mathematical Monographs*, Vol. 65 (American Mathematical Society, Providence, 1986).